NAS5-25871

DRD/GODDARD

FINAL REPORT FOR:
SOLAR OPTICAL TELESCOPE
PRIMARY MIRROR CONTROLLER

DR. RICHARD J. BROWN
DR. DANKAI LIU

THE NAVTROL COMPANY
9204 MARKVILLE
DALLAS, TEXAS 75243

(NASA-CR-174416) SOLAR OPTICAL TELESCOPE PRIMARY MIRROR CONTROLLER Final Report, Sep. 1979 - Aug. 1980 (Navtrol Co., Dallas, Tex.) 114 p HC A06/MF A01 CSCL 03A

N85-19903

Unclas
G3/89 18118

FINAL REPORT FOR PERIOD
SEPTEMBER, 1979 - AUGUST, 1980

PREPARED FOR:
GODDARD SPACE FLIGHT CENTER
GREENBELT, MARYLAND 20771

TABLE OF CONTENTS

Section	Title	Page
1.0	INTRODUCTION	1-1
2.0	TECHNICAL APPROACH	2-1
2.1	CONTROL APPROACH	2-1
2.1.1	GENERAL DISCUSSION	2-1
2.1.2	OVERALL CONTROL APPROACH	2-5
2.1.3	TRANSFORMATION DISCUSSION	2-12
2.1.4	ACTUATOR LINK CONTROL LOOP DESIGN	2-17
2.2	HARDWARE DESCRIPTION	2-28
2.2.1	DIGITAL CONTROLLER DESCRIPTION	2-28
2.2.1.1	INTRODUCTION	2-28
2.2.1.2	DIGITAL CONTROLLER PROCESSOR UNIT	2-28
2.2.1.2.1	PROGRAM MEMORY EXPANSION	2-28
2.2.1.2.2	DATA MEMORY REFERENCED BRANCHING	2-29
2.2.1.2.3	DATA MEMORY EXPANSION	2-19
2.2.1.2.4	INDEXING CHANGE	2-30
2.2.1.2.5	ALU-ACCUMULATOR MODIFICATION	2-31
2.2.1.2.6	INDIRECT ADDRESSING AND MEMORY 2	2-32
2.2.1.2.7	PRINTED CIRCUIT BOARD MECHANIZATION	2-32
2.2.2	MOTOR-ENCODER INTERFACES	2-33
2.2.2.1	ENCODER INTERFACE	2-33
2.2.2.2	MOTOR DRIVE AMPLIFIER	2-38
2.2.3	ACTUATOR CONTROL	2-44
2.2.4	SERVO DEVELOPMENT SYSTEM	2-48
3.0	RESULTS	3-1
3.1	ANALYSIS AND SIMULATION RESULTS	3-1
3.1.1	TRANSFORMATION RESULTS	3-1
3.1.1.1	PRECISION TRANSFORMATION	3-1
3.1.1.2	"FAST" TRANSFORMATION	3-3
3.1.1.3	ERROR SENSITIVITY ANALYSIS	3-6
3.1.2	ACTUATOR CONTROL LOOP ANALYSIS	3-13
3.2	COMPUTER PROGRAM DEFINITION	3-30
3.2.1	MEMORY ALLOTMENT	3-30
3.2.2	TIMING RESULTS	3-33
3.3	HARDWARE RESULTS	3-37
3.3.1	COMPUTER RESULTS	3-37

Table of Contents (Cont.)

Section	Title	Page
3.3.2	ACTUATOR CONTROL RESULTS.....	3-37
3.3.3	ACTUATOR ASSEMBLY BACKLASH TESTS.....	3-42
3.3.4	MOTOR ENCODER INTERFACE RESULTS.....	3-42
4.0	CONCLUSIONS AND RECOMMENDATIONS.....	4-1
4.1	CONCLUSIONS.....	4-1
4.2	RECOMMENDATIONS.....	4-3

APPENDICES

A. ALL DIGITAL CONTROLLER TECHNICAL DESCRIPTION

B. BALDWIN ENCODER SPECIFICATION

C. DIGITAL CONTROLLER DATA MEMORY ASSIGNMENT

D. TRANSFORMATION TESTING RESULTS

LIST OF TABLES

Table No.	Title	Page
2.1-1	SOT LINK COORDINATE DATA	2-3
2.1-2	RANGE OF DATA INPUT	2-3
2.1-3	ACTUAL TRANSFORMATION	2-15
2.1-4	"PRECISION" TRANSFORMATION	2-16
2.2-1	SOT APM TORQUE MOTOR	2-46
2.2-2	SOT APM TACHOMETER	2-47
3.1-1	"PRECISION" TRANSFORMATION RESULTS	3-2
3.1-2	"FAST" TRANSFORMATION	3-5
3.1-3	RATE TRANSFORMATION RESULTS	3-7
3.1-4	SENSITIVITY MATRICES	3-8
3.1-5	EFFECT OF ACTUATOR ON MIRROR POSITION	3-10
3.1-6	PARAMETERS FOR ACTUATOR CONTROL RUNS	3-16
3.2-1	PROGRAM MEMORY ALLOCATION	3-31
3.2-2	SOT COMPUTATIONAL TIME REQUIREMENT	3-34
3.3-1	SOT COMPUTER DEFINITION	3-38

LIST OF FIGURES

Figure No.	Title	Page
2.1-1	CONTROL APPROACH FOR THE SOT APM.....	2-6
2.1-2	DETAILS OF SOT APM CONTROL APPROACH.....	2-11
2.1-3	REFERENCE COORDINATE SYSTEM	2-14
2.1-4	SOT STRUCTURAL MODEL.....	2-19
2.1-5	SECOND ORDER EXAMPLE.....	2-21
2.1-6	ACTUATOR LOOP CONTROL APPROACH USING TACH FEEDBACK.....	2-26
2.2-1	ENCODER I/F BLOCK DIAGRAM.....	2-35
2.2-2	MOTOR DRIVE AMPLIFIER FUNCTIONAL BLOCK DIAGRAM.....	2-40
2.2-3	SOT POWER AMPLIFIER.....	2-43
2.2-4	SOT APM ACTUATOR ASSEMBLY.....	2-45
3.1-1	LINK CONFIGURATION.....	3-11
3.1-2	SOT ACTUATOR DYNAMIC MODEL INCLUDING STRUCTURAL MODE.....	3-14
3.1-3	ACTUATOR LOOP CONTROL APPROACH USING TACH FEEDBACK.....	3-15
3.1-4A	12.6 HZ LOOP WITH TACH FEEDBACK.....	3-17
3.1-4B	12.6 HZ LOOP WITH TACH FEEDBACK.....	3-18
3.1-5A	12.7 HZ WITH TACH FEEDBACK.....	3-19
3.1-5B	12.7 HZ WITH TACH FEEDBACK.....	3-20
3.1-6	12.9 HZ LOOP WITH TACH FEEDBACK.....	3-21
3.1-7	12.9 HZ LOOP WITH TACH FEEDBACK BUT LOW INERTIA.....	3-23
3.1-8	12.6 HZ LOOP WITH TACH FEEDBACK(Low J)	3-24
3.1-9	12.6 HZ. LOOP WITH TACH FEEDBACK(OFFSET)	3-26
3.1-10	6.3 HZ LOOP WITH TACH FEEDBACK(100°STEP)	3-27
3.1-11	12.9 HZ LOOP WITH TACH FEEDBACK(J=19X)..	3-29
3.2-1	DATA MEMORY ALLOCATION.....	3-32
3.2-2	SOT CONTROL PROGRAM SEQUENCE	3-35

LIST OF FIGURES (Cont.)

Figure No	Title	Page
3.3-1	POSITION ERROR FOR 1° POSITION STEP COMMAND..	3-40
3.3-2	FOLLOW UP MODEL POSITION ERROR FOR 1° POSITION COMMAND.....	3-40
3.3-3	POSITION ERROR FOR 100° POSITION COMMAND.....	3-41
3.3-4	FOLLOW UP MODEL POSITION ERROR FOR 100° POSITION COMMAND.....	3-41
3.3-5	POSITION ERROR FOR 100°/s VELOCITY STEP COMMAND.....	3-43
3.3-6	FOLLOW UP MODEL POSITION ERROR FOR 100°/s VELOCITY STEP COMMAND.....	3-43
3.3-7	VELOCITY ERROR FOR 100°/s VELOCITY STEP COMMAND.....	3-44
3.3-8	FOLLOW UP VELOCITY ERROR FOR 100°/s VELCOITY STEP COMMAND.....	3-44
3.3-9	BACKLASH TEST RESULT.....	3-45
3.3-10	BACKLASH TEST SETUP.....	3-46

SECTION I
INTRODUCTION

The object of the program discussed in this report was to develop control techniques and a capability for control of the Articulated Primary Mirror (APM) of the Solar Optical Telescope ISOT). The primary mirror is large, 1.25 meters in diameter, and weighs about 800 kg. Six linear actuators provide both control and support, with termination at the mirror periphery. Control of the length of each of these actuators makes it possible to move the mirror with 6 degrees of freedom. The required control involves both translational and rotational control over small angles and small displacements with severe requirements on stability and accuracy.

The implementation of the control law resolving commands to the 6 diagonal linear actuators was a primary part of this program. Implementation implies not only developing the algorithms but fitting these into a computer, defining requirements both for memory and timing for that computer.

The program was to be one step in implementing a full scale mock up of the APM. The APM with 6 actuators was to be constructed at the Sacremento Peak Observatory under the direction of Dr. Richard Dunn while Navtrol provided the electronics and the control implementation. The mock up would permit complete testing and evaluation

of various control components, concepts and techniques, so that the space qualifiable system would meet the various stringent requirements imposed on it with a minimum of problems.

It is shown in the attached report that the All Digital Controller, developed for the NASA Goddard Space Flight Center for just such an application, can perform all the functions defined thus far for control of the APM with considerable margin to spare. This extra capability could be used in performing other functions. The Processor Unit, capable of handling all the SOT computation, including the complex transformations and control of all 6 actuators, is contained on 3 double sided printed circuit boards approximately 5.6 x 10" in size. (This does not include the interface modules.) Six Motor-encoder interface modules are required which can be located adjacent to actuators which they control.

In the sections that follows the implementation is described, and the rational for selecting such an implementation provided. The result of the implementation on the hardware configuration, along with various interface requirements is presented.

Navtrol feels most fortunate for having worked with the NASA Goddard Space Flight Center in the development of the All Digital Controller System. The SOT program reported on here demonstrates the capability

of the All Digital Controller to meet yet another application. It further demonstrates that the faith exhibited by NASA GSFC in funding the development of a general purpose digital controller applicable to many applications was not misguided. Navtrol wishes to acknowledge the guidance and help of Mr. Phil Studer who initiated the original ADC development program within NASA and has been associated with the Digital Controller ever since. Navtrol also wishes to acknowledge technical and other assistance provided on the SOT program from such people as Ewald Schmidt, Pete Hui and Bob Fulcher of NASA and Dr. Dick Dunn of the Sacremento Peak Observatory.

SECTION II
TECHNICAL APPROACH

2.1 CONTROL APPROACH

2.1.1. GENERAL DISCUSSION

As indicated in the Introduction, the object of the program discussed in this report was to develop a control technique and capability for control of the Articulated Primary Mirror (APM) of the Solar Optical Telescope (SOT). The primary mirror is large (1.25 meters in diameter) and heavy (800kg). Six linear actuators provide both control and support, with termination at the mirror periphery. Control of the length of each of these actuators makes it possible to move the mirror with six degrees of freedom. The required control involves both translational and rotational control over small angles and displacements with severe requirements on stability and accuracy.

The program reported here, by Nav:trol, was only one of several to define the control approaches and techniques as well as the over all configuration of the Solar Optical Telescope. Based on results of these studies and various technical discussions, it was decided that control of the mirror should be defined about the conic foci. Rotation about the conic foci results in an equal angular rotation of the line of sight direction of the telescope. This was appealing even through rotation about the conic foci required both rotation and translation

of the mirror surface. The intermix of rotation and translational motions for a rotational command is of little consequence since all motion of the mirror occurs as a result of adjustment in length of the six extendable links supporting the mirror. Viewing the control actuation of a single link provides little or no insight as to the type of motion, angular or linear, being commanded at the mirror surface.

For the program reported here it was assumed that all measurements are made with respect to the conic foci. Five sensors are assumed. These measure error in linear displacement, x, y and z, and rotational motion about the x and y axis. A right handed coordinate system was assumed with the x and y axis parallel to the mirror surface but originating through the conic foci. The z axis originates at the conic foci and extends down through the center of the mirror.

Table 2.1-1 defines the coordinates of each of the links for the configuration used in this program. Table 2.1-2 defines the range of data input expected from each of the 5 sensors. Roll motion about the z axis, indicated by θ_z, is not measured by any sensor nor is it a critical parameter to be controlled. However, roll must be controlled in either an implicit or explicit manner for if it is not controlled, truncation, round off and other errors will cause the mirror to slowly rotate until the links are

TABLE 2.1-1

SOT Link Coordinate Data

(RCVD 10/2/79 from NASA GSFC)

	Base Coordinates			Mirror Coordinates		
Link	X_b	Y_b	Z_b	X_m	Y_m	Z_m
L_1	-60.228	34.772	485.030	-57.254	23.673	475.389
L_2	-60.228	-34.772	485.030	-57.254	-23.673	475.389
L_3	0.000	-69.545	485.030	8.126	-61.420	475.389
L_4	60.228	-34.772	485.030	49.128	-37.747	475.389
L_5	60.228	34.772	485.030	49.128	37.747	475.389
L_6	0.000	69.545	485.030	8.126	61.420	475.389

All dimensions in cm.

TABLE 2.1-2: Range of Data Input

Input Parameter	RFP Specified Range	RFP Specified Rate	
		Raster & Focus	*IMC
DXC	± 3cm.	-	-
DYC	± 3cm.	-	-
DZC	± 1cm.	1 mm/sec	-
Θ_x	± .5deg.	1 deg/min.	1.05 deg/min.
Θ_y	± .5deg	1 deg/min.	1.05 deg/min.
Θ_z	± 0 deg.	0	0
			* ± 1 arc sec. @ 10 Hz.

extended to their full lengths and control of other parameters is impeded. If 6 degrees of freedom are provided then 6 degrees of freedom must be controlled. The control approach recommended by Navtrol in the following paragraphs provides for very tight control of roll as well as the other parameters. In the control approach taken it would be difficult to provide for loose control of roll while providing tight control of other parameters.

The transformation from motion about and translation with respect to the conic foci to changes in length of the six extendable links is both non-linear and complex. If the line of sight of telescope is to be tightly controlled, fast and accurate transformation of line of sight errors to adjustments in length of each extendable link is required. High frequency image motion compensation dictated the requirement of a specialized, very high capability digital computer, applicable to control situations. The Digital Controller developed by Navtrol under contract with NASA Goddard Space Flight Center is such a machine. It can handle the precision transformation required at a rate of 128 times per second, provide precision control of the 6 extendable link actuators 256 times per second and still have considerable capacity for many other tasks. It is described in detail in the following sections and in Appendix A.

Early concepts about the control of the Solar Optical Telescope primary mirror involved the use of stepper motors for controlling the length of the extendable links. By the time Navtrol commenced the program reported here, the use of linear torque motors with appropriate feedback was being held as being more flexible and offering the promise of higher performance then use of stepper motors. The possibility of dropped steps resulting in slow build up of errors, especially in roll, plus the improved dynamics offered by linear torque motors was the reason for their selection.

2.1.2 OVERALL CONTROL APPROACH

In the program reported here an overall control approach for the Solar Optical Telescope (SOT) Articulated Primary Mirror (APM) was defined which should provide excellent results for both open and closed loops modes of operation. The apporach goes well beyond that which has previously discussed by various contractors in that it provides both control of the roll axis and open loop capability. This approach is illustrated on Figure 2.1-1.

The innermost loop, of which there are six, involves control of the length of the extendable links by use of the link mounted motors and encoders. This inner control loop controls the actual link length to the desired or "target" length. The "target" link length estimator is updated at rates up to 128 times per second using information

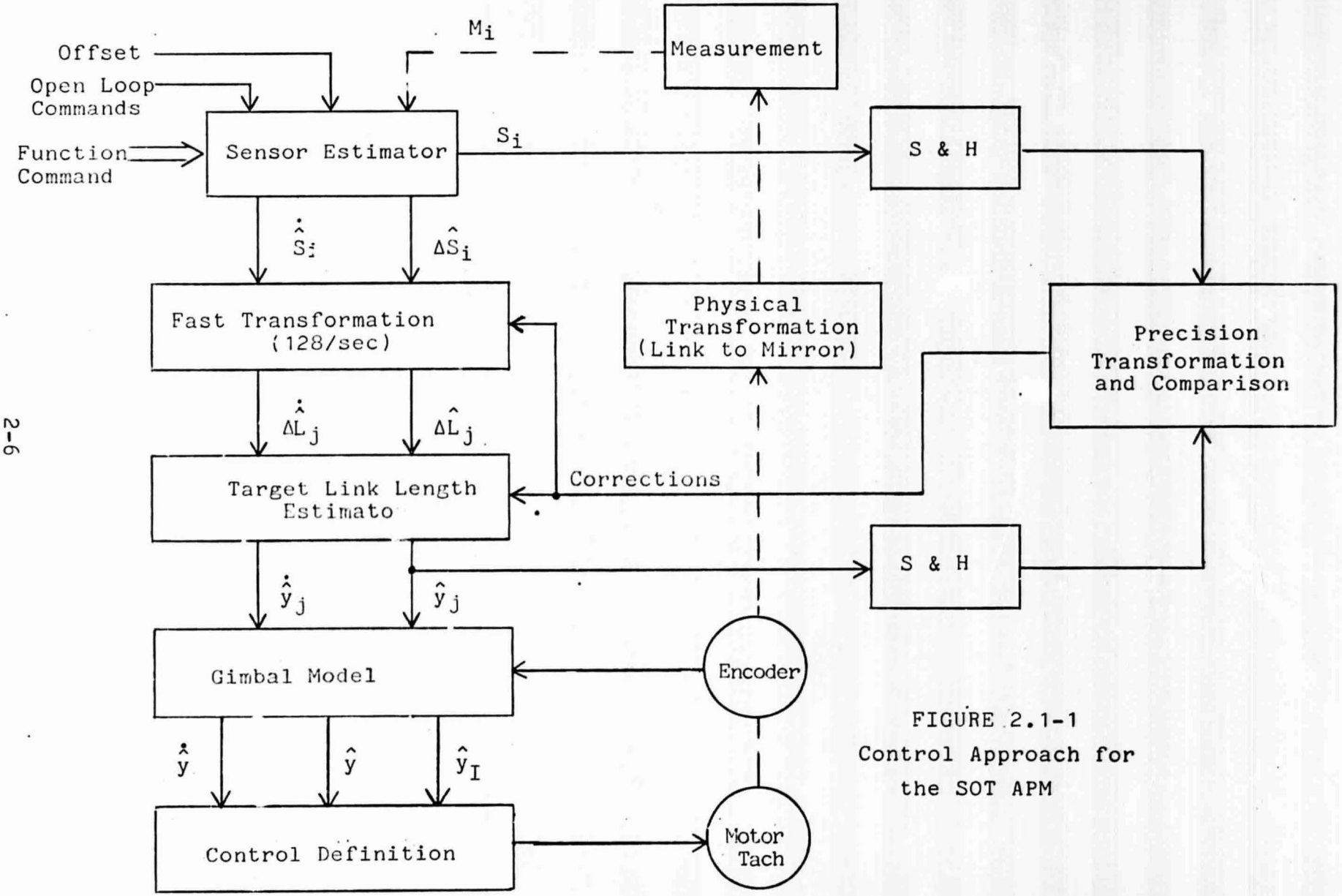

FIGURE 2.1-1
Control Approach for the SOT APM

obtained from the sensors and passed through the "Fast Transformation" in the illustration of Figure 2.1-1, delta positional corrections, Δs_i, are passed through the fast transformation as well as the sensor rate estimate. Change in position may appear redundant to velocity but is not because of the way that offsets and change in position commands are handled. Steps, for example, would require rate impulses of infinite height and so are not handled by simple rate transformations. The corrected target link estimator in turn provides the position and rate to which the link actuators are slaved. In this "inner loop" a sampling rate of 256 samples/second is used.

If measurements were made in all six axes and no open loop capability was required the "Fast Transformation" functions alone, without additional corrections, would be sufficient to provide control. Any error build up in the Fast Transformation or integration would be measured by the sensors and integrated out by the overall closed loop control system. This is similar to control approaches advocated in previous studies. However, no measurements are made on roll and truncation, round off and other error sources could cause the mirror to slowly rotate in roll until the links are extended to their full lengths and control of other parameters is impeded. In addition, over the expected angular and translational excursions of the mirror the "Fast Transformation" changes considerably and can not be considered a constant transformation.

Therefore some means of updating it must be included in the algorithms either from tabulated data or calculations.

To prevent roll build up from occurring and to correct the fast transformation loop, another path, a "Precision Transformation and Correction" path, is provided. This path includes a precision transformation from the nominal or zero reference position of the mirror to the desired mirror position, defining each link length required. The transformation is always made with respect to the "zero reference position" so there is no possibility of build up in errors in roll or any other axis. Since any combination of mirror motion can be commanded, without measurements being made by the sensors, a full "open loop" capability is provided. In this "open loop" mode mirror orientation is defined solely by the measured lengths of the actuator links.

For roll the total angle will always equal approximatley zero For the other two angles and for linear motion in x, y and z, estimates of the desired total displacement will be computed by the ADC computer. Knowing the full angular and translational offsets, the precise change in link length from nominal for each of the links can be calculated. Since relatively large angles, 0.5^{o}, are transformed, correction for higher order effects and double precision are required.

Because of the amount of calculation that is involved in the "precision transformation and comparison" function, it was originally planned to spread the calculations out over many cycles of the inner and fast transformation loop.

With the inner loop providing only corrections, a rate of about 8 times per second could probably be tolerated. However, it was shown that the program could be considerably simplified and performance improved by performing the precision transformation 128 times per second. This eliminates the need for passing changes in position through the fast transformation, reserving its use only for rate in the set of algorithms adopted. The high performance capability of the All Digital Controller permits this approach to be taken without jeopardizing other functions that the All Digital Controller must perform.

To perform the precision transformation and correction, data from all 5 sensors and 6 actuator links must be "sampled" at approximately the same instant of time. (Sensor information is only comparable to link lengths at the same instant of time.) This simultaneous sampling requirement is indicated on Figure 2.1-1 by the sampling and hold (S and H) functions. A precision transformation of the sensor information is then made to provide the desired length link and this is compared to the stored link lengths. The differences are then used to provide correction to the target link length estimator. Using the same information, corrections are made to the fast transformation so that cross coupling terms are kept to a minimum.

A question which might be asked is: If the precision estimator is so accurate why use a target link length

estimator? The target link length estimator provides interpolation and extrapolation using rate and last known position to provide control of the actual actuators at a rate of 256 times per second, twice the transformed update rate. Interpolation and extrapolation is also required since the measurement of all 6 actuators and 5 sensors cannot be made simultaneously. By use of estimated rates, positions can be extrapolated or interpolated to the same instant of time.

Figure 2.1-2 provides additional functional details of the SOT APM control approach. As indicated, two states are allocated for sensor estimation. The figure illustrates the calculation for only one sensor measurement, rotation about the x axis or $\Delta\theta_x$. It is assumed that the sensor measures only the offset away from the desired pointing direction, rather than the total angle. This measurement is fed through a pair of Kalman gains, K1 and K2 to update the two states of the sensor estimator. The "Kalman" gains can be selected on the basis of bandwidth or on the statistical characteristics of the measurement and associated disturbances. Although a momentary build up of error in integration to obtain $\hat{\theta}_x$ can occur due to computational limitations of the computer, these will be bounded to within acceptable levels by use of the multiple control loops previously described. If $\hat{\theta}_x$ does not represent the actual θ_x it will offset the mirror

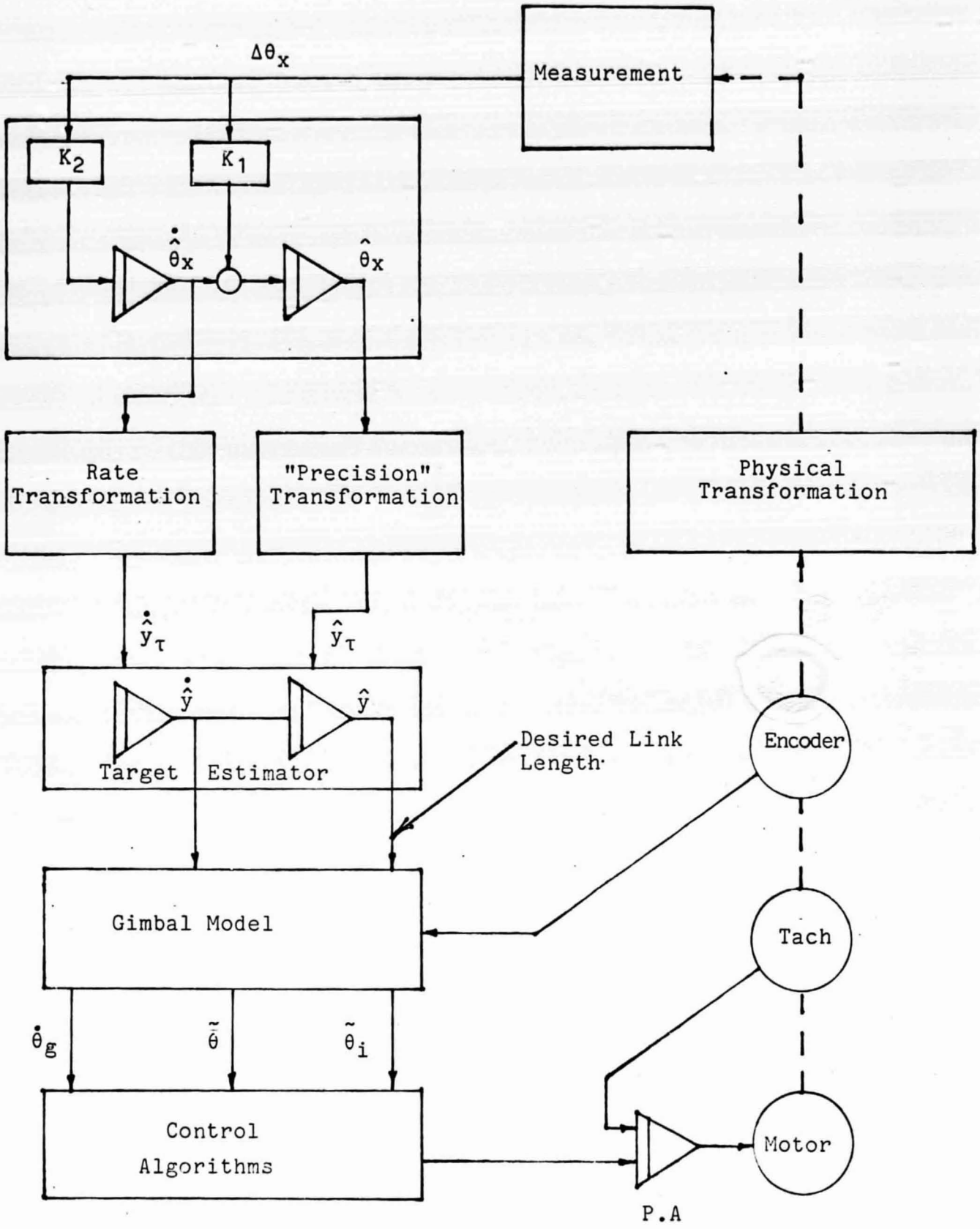

FIGURE 2.1-2: Details of SOT APM Control Approach

resulting in a measurement offset and a correction to $\hat{\theta}_x$.

Again note that the measurements represent error rather than total displacement angle while the estimator estimates the total displacement angle. The total angle must be estimated since this is required for the "zero based" precision transformation.

Referring to Figure 2.1-2, open loop control can be provided by commanding a θ_x and comparing $\hat{\theta}_x$ to it. By subtracting $\hat{\theta}_x$ from θ_x a synthetic measurement is provided which can be utilized in exactly the same manner as previously discussed. Very accurate open loop control is achieved in this manner.

2.1.3 TRANSFORMATION DISCUSSION

Although definition of the transformation from sensor error to link length was originally not a part of this program, to prevent delays to the program that could not be recovered Navtrol defined this transformation. The derivation of this transformation took advantage of conversations held with Mr. Pete Hui at NASA. A computer program was written which defines: 1) the actual transformation, 2) an accurate approximation of the transformation referred to as the "Precision Transformation" and 3) "Fast Transformation" which is only accurate for small perturbations about its referenced position. The transformations are general and apply for any given set of platform link coordinates.

The reference coordinate system for these transformations is illustrated on Figure 2.1-3. As indicated, the center of the reference coordinate system is the conic foci. The positive Z axis extends from the conic foci through and perpendicular to the base which supports the mirror through the 6 actuators links. The diagram illustrates the assumed positive rotation for angles.

Table 2.1-3 provides the derived "actual" Transformation from sensor offsets to length of actuator links. The set of equations must be exercised 6 times, once for each of the 6 actuator links. Roll angle does not appear in the trnasformation since it is assumed to be zero. The transformation shown is only accurate as long as θ_z is zero. However, transforming using the total sensor displacements to the total actuator length results in mirror motion in which roll angle is zero, or at least very nearly.

Table 2.1-4 illustrates the "Precision Transformation" utilized in the Digital Controller algorithms. The precision transformation takes advantage of the fact that the sine and cosine of an angle can be obtained by a power series with the first few turns providing sufficient accuracy for small angles. In the equations presented, all terms above second order were excluded. The algorithms also make use of an approximation for the square root thereby saving additional computation time. These equations have been shown to provide excellent agreement with the "actual transformation" in large scale computer simulation studies.

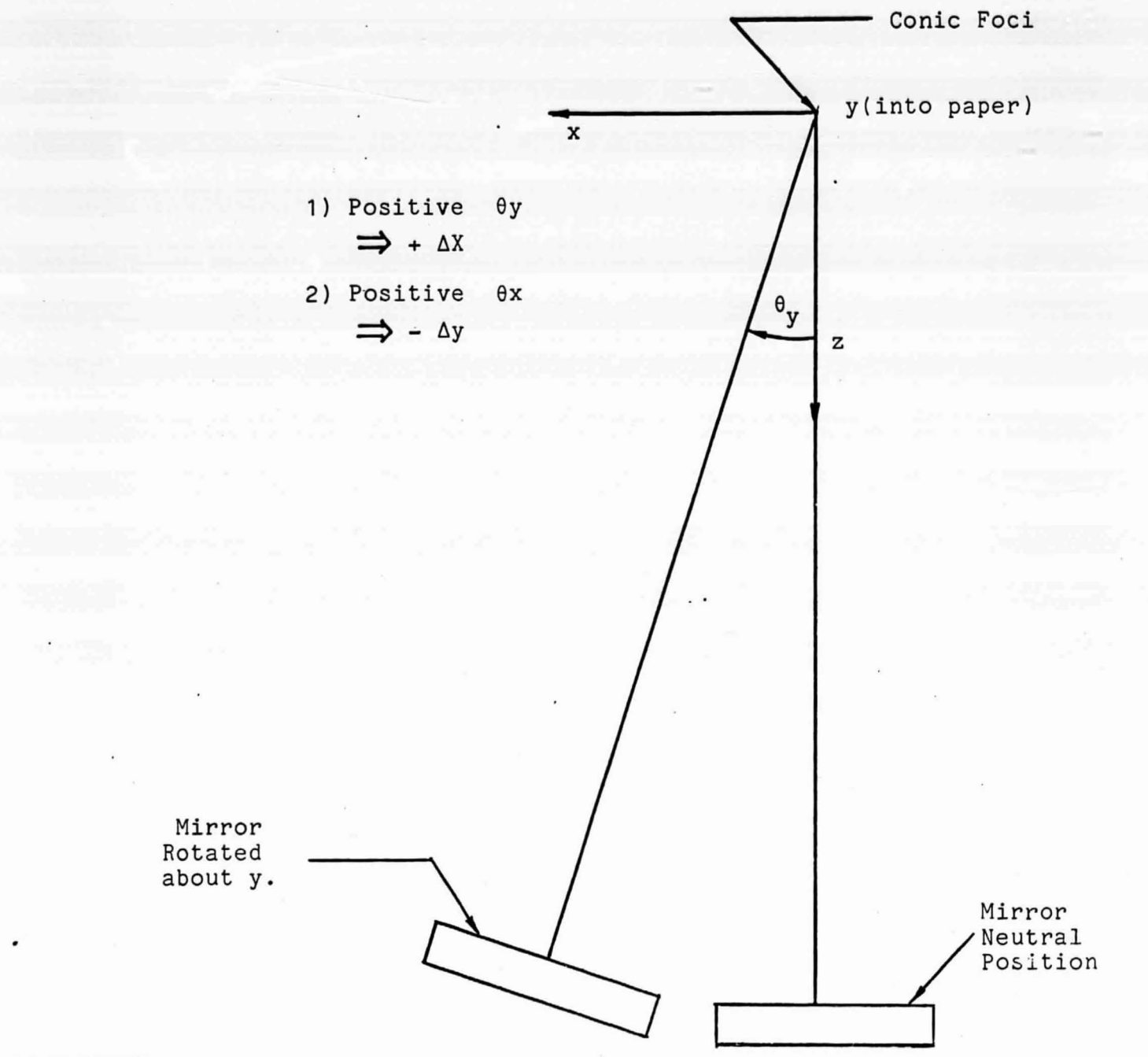

FIGURE 2.1-3: Reference Coordinate System

TABLE 2.1-3 : Actual Transformation

XM(i), XMA(i) YM(i), YMA(i) ZM(i), ZMA(i)	Initial and final coordinates at mirror connection of link (i).
XB(i) YB(i) ZB(i)	Coordinates at base connection of link (i).
AL(i), ALA(i):	Initial and final link length
DXC, DYC, DZC:	Translational motion of mirror
Θ_x, Θ_y:	Angles of rotation about x and y axes respectively.

$$XMA(i) = XM(i) * \cos \Theta_y + YM(i) * \sin \Theta_y * \sin \Theta_x + ZM(i) * \sin \Theta_y * \cos \Theta_x + DXC$$

$$YMA(i) = YM(i) * \cos \Theta_x - ZM(i) * \sin \Theta_x + DYC$$

$$ZMA(i) = -XM(i) * \sin \Theta_y + YM(i) * \cos \Theta_y * \sin \Theta_x + ZM(i) * \cos \Theta_y * \cos \Theta_x + DZC$$

$$XDA(i) = XMA(i) - XB(i)$$

$$YDA(i) = YMA(i) - YB(i)$$

$$ZDA(i) = ZDA(i) - ZB(i)$$

$$ALA(i) = \sqrt{XDA^2(i) + YDA^2(i) + ZDA^2(i)}$$

$$DL(i) = ALA(i) - AL(i)$$

TABLE 2.1-4: "Precision" Transformation

DX(i)
DY(i)
DZ(i)
} Change in coordinates at mirror connection of link (i).

DL(i) = Adjustment required in length of actuator.

ALM(i) = Measured length of link (i).

ALN(i) = Length of link (i) with mirror at the "zero" position.

$$DX(i) = (-.5 * \theta_y^2) * XM(i) + (\theta_y * \theta_x) * YM(i) + \theta_y * ZM(i) + DXC$$

$$DY(i) = (-.5 * \theta_x^2) * YM(i) - \theta_x * ZM(i) + DYC$$

$$DZ(i) = (-\theta_y) * XM(i) + (\theta_x) * YM(i) - .5 * (\theta_y^2 + \theta_x^2) * ZM(i) + DZC$$

$$XD(i) = XM(i) - XB(i)$$

$$YD(i) = YM(i) - YB(i)$$

$$ZD(i) = ZM(i) - ZB(i)$$

$$DXA(i) = XD(i) + .5 * DX(i)$$

$$DYA(i) = YD(i) + .5 * DY(i)$$

$$DZA(i) = ZD(i) + .5 * DZ(i)$$

$$ALMA(i) = (ALM(i) + ALN(i)) * .5$$

$$DL(i) = \left[DXA(i) * DX(i) + DYA(i) * DY(i) + DZA(i) * DZ(i)\right] / ALMA(i)$$

$$*DL(i) = DL(i) * \left(\frac{ALMA(i)}{ALN(i) + DL(i)/2.}\right)$$

* This correction, although it improves the answer, is thought to be not needed and is not in the present algorithms.

The fast transformation is derived in a manner similar to the precision transformation except that terms above first order have been eliminated. However, this transformation is defined with a nominal at the actual position of the mirror at the time the corrections were made. The frequent update insures that the deviations about the referenced position will be quite small so that a very accurate transformation is made for sensor rate to that of the actuator links. The fast transformation is also computationally efficient.

The fast Transformation is also convenient for expressing the sensitivity of the link lengths in terms of errors at the sensor. Since it is a true matrix it can be inverted to obtain the sensitivity of the mirror to small errors in actuators links. These sensitivities are further discussed and results provided in Section 3 of this report.

2.1.4 ACTUATOR LINK CONTROL LOOP DESIGN

At the initiation of the study it was assumed that 10 Hz loops would be adequate for control of the 6 actuator links of the SOT APM. Friction levels and other sources of disturbance torques had not been defined at that point. Early in the program, a review, of documents indicated that a friction level of 1.25 lb. in. was expected. The approach planned at that time for the actuator loops was for use of second order system with the 10 Hz bandwidth and a damping

factor of 1. A Kalman filter for each of the gimbal loops was to be utilized to obtain velocity information for stablizing the system and a frictional estimate to improve accuracy. Integral control was also to be included. However, simulation results showed the gain associated with a 10 Hz loop was insufficient to overcome a friction level of 1.25 lb. in. and provide the desired accuracy of .1 arc seconds at the platform.

Although integral compensation and friction estimator brought the offset error down with time it did not appear that the dynamics were adequate. To improve dynamics the bandwidth of the inner loop was increased to 25 Hz. The increase in bandwidth not only provided a 6.25 increase in wide bandwidth gain, but also provided improved dynamics for the integral gain and friction estimation locps. However, the 25 Hz tended to excite the 50 Hz resonance of the mirror actuator assembly in spite of the considerable isolation provided by the ball and screw configuration. Friction tended further to diminish the feedback of mirror motion to the encoder but the problem remained. To control it, the 50 Hz structural mode was included in the processor Kalman filter model used in the actuator control system. With this configuration performance was much improved.

Figure 2.1-4 illustrates the gimbal model used both in the Digital Controller Kalman filter, for the approach just described (which was later discarded),

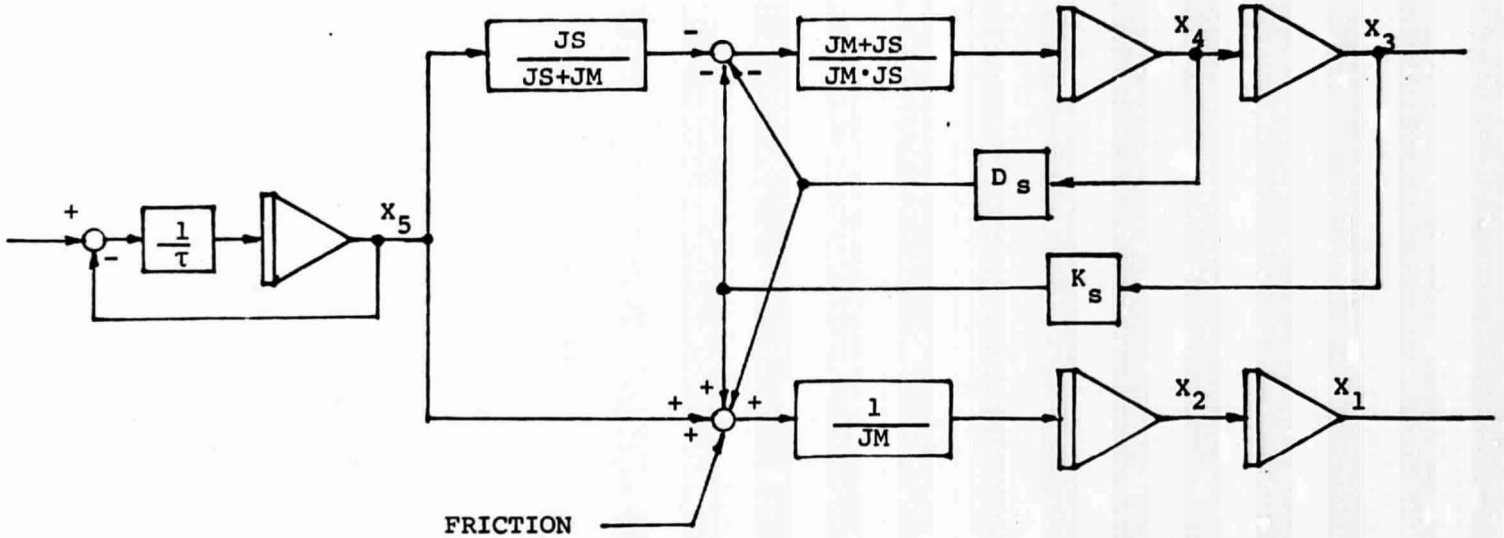

FIGURE 2.1-4: SOT STRUCTURAL MODEL

and as a model of the actual system in simulation studies for both the approach just described and the control approach which was finally selected. The state x_1 represents motor angle while x_2 represents motor rate. The states x_3 and x_4 are states of the structural mode resonance with x_3 defined as the difference angle between the two ends of the "structural mode spring." The state, x_5 represents the power amplifier motor time constant which must be included in simulations of wide bandwidth systems. Although the PA is nominally a current drive amplifier, infinite voltage is not available so that torque is not instaneously available. Unfortunately, the time constant depends on the torque value and whether torque is increasing or decreasing in magnitude. This was modeled to a reasonable extent but the model was not perfect.

It was further shown that an increase in inertia provided a reduction in error of about the same ratio as the inertia was increased, providing that the loop bandwidth was kept constant. Increasing the inertia results in a redistribution of gain (for constant bandwidth loop) so that the same error provides increased torque to overcome friction. This is illustrated on Figure 2.1-5. Here the inertia is increased 10:1 from 0.0137 to 0.137 lb. in^2. It is shown that for a second order loop, an offset angle of .1 degree results in a torque of .59 in. lb.

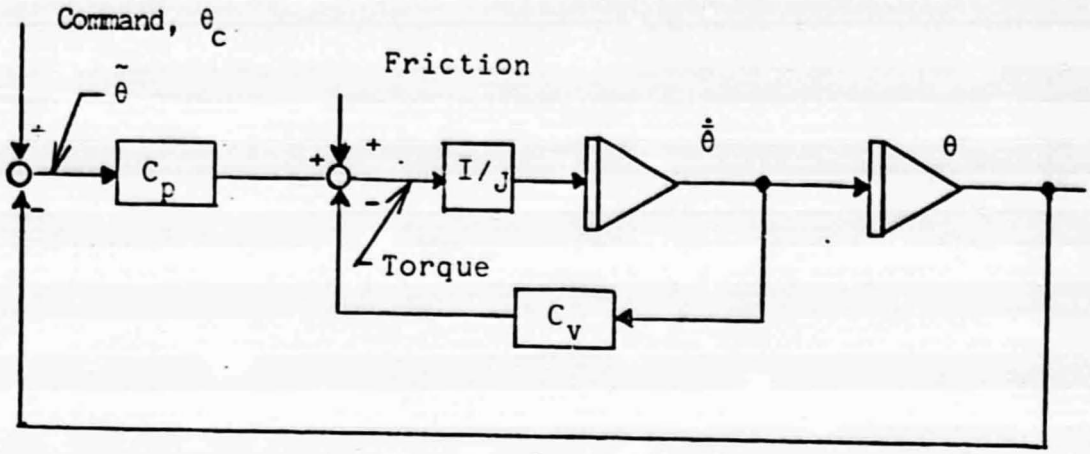

$$\theta/\theta_c = \frac{C_p}{s^2+(c_v/J)s + {}^{C_p}/_J}$$

If $C_p = (\omega_n{}^2)J$, $C_v = 2\xi\omega_n J$ then:

Poles are:

$$S = -\omega_n(\xi \mp \sqrt{\xi^2-1})$$

J_s = .0137 in lb. sec.^{2} ("small inertia")

J_l = .137 in. lb. sec.^{2} ("large inertia")

If fn = 25Hz ω_n = 157 r/s

$T = C_p \cdot \tilde{\theta}$ $\begin{cases} C_p = 338 \text{ for } J_s \\ C_p = 3380 \text{ for } J_l \end{cases}$

If ω_n = 25 Hz$\cdot(2\Pi)$ $\tilde{\theta}$ = .1 degree

T = .59 in. lb. for J_s

T = 5.9 in. lb. for J_l

FIGURE 2.1-5: Second Order Example

for the small and 5.9 in. lb. for the large inertia. The use of integral gain and friction estimation will reduce the indicated errors still further.

For a fixed size torque motor increasing the inertia decreases the amount of acceleration available. If this is not a problem, increasing the inertia permits an increase in gain without a subsequent increase in bandwidth. Loop bandwidth is limited by the sampling rate which a single All Digital Controller could accomodate, but also by the excitation of the structural mode. With the above increase in inertia it was shown that a 65 lb. in. torque motor provided sufficient torque to insure the .1 arc second accuracy with dynamic motion as specified in the NASA RFP (1 arc second at 10 Hz). The increase in inertia also improves the isolation of the motor/encoder loop from platform motion The loop, with the structural mode in the model and with an 8:1 increase in inertia provided good performance and tolerance to shifts in the frequency of the structural mode appeared to be adequate.

About this time it was determined that a friction level of 8 lb. in. was more realistic. Although it appeared that even with the new friction level a good chance of meeting the performance critera remained, it was decided to pursue an approach which offered better performance and lower risks. Dr. Dick Dunn of the Sacramento Peak Observatory suggested a very tight tach loop as a way of

overcoming the effect of friction. The high gain tach loop effectively lowers the gain in the forward displacement loop so that displacement gain can be increased while maintaining the bandwidth within the desired limits. Computational time requirements place a sampling limitation for a single All Digital Controller which prevents the very wide bandwidth rate loop from being implemented within the All Digital Controller. In addition, the resolution limitation of the encoder is such as to make it unusable for wide bandwidth rate applications. The approach could be implemented digitally if additional encoder bits were provided and if the use of a second digital controller was permitted. It was felt that a more reasonable approach was the addition of a good tachometer with the rate loop closed outside the All Digital Controller.

The new approach required considerable changes in the work already accomplished up to that time period, not only in the area of loop analysis but also in the design of the power amplifier. However, advantages seem to offset disadvantages. Advantages are:

1) Close physical association of tachometer and motor permits use of the best method found yet to reduce the effect of non-linearities, that of use of a very tight feedback loop around the non-linearities
2) Use of the wide bandwidth tach loop enables the displacement loop to operate at a lower bandwidth

(a bandwidth of about 12.8 Hz was selected) greatly reducing the possibility of excitation of structural modes, not only in the vicinity of the actuator mirror area but also in the structure between the actuator, the IPS system and the sensors as well.

3) The narrow bandwidth reduces the computational load on the All Digital Controller providing time to perform many additional tasks.

The structural mode consideration was probably the overwhelming one since Navtrol, along with others, feel this could be a major risk area in the design of the overall Solar Optical Telescope control system. By using the tach to overcome friction levels, bandwidths could be reduced further, if need be, in order to keep from exciting the structural modes and still meet the basic accuracy requirements of SOT.

The implementation of a high gain tachometer loop around the amplifier-torque motor eliminates the necessity for (and render very difficult) the complete modeling of gimbal dynamics within the ADC computer. However, commands to the power amplifier must be limited to lie within the capabilities of the torque motor, tach, encoder and other elements of the loop. It is also desirable to minimize the excitation of the structural modes.

Fi[illegible] 2.1-6 illustrates the approach selected to accomplish these goals for the actuator loop configuration using tach feedback. The approach is similar to the model reference approach used in design of flight control systems whereby the system is forced to follow an "idealized" response from the model system. The "model system" on Figure 2.1-6 consists of states y_{1f}, y_{2f} and y_{3f} and is referred to, within Navtrol, as the follow up system. The inputs to this system are the desired actuator link length $\hat{y}_1$ and the desired link velocity $\hat{y}_2$. These come from the "target estimator" previously described which is corrected 128 times per second from the Precision and Fast Transformations of displacements and rates of the 5 sensors. The follow up filter is structured to provide minimum time response from one angle to another within the constraints of torque limited to 64.5 in. lb. and velocity limited to 650 $^{o}/_{s}$ at actuator. The filter has a linear response region and within this the filter rolls off at about 15 Hz minimizing excitation of presently known body modes. Velocity from the follow up system is fed forward through appropriate gains to command the same velocity from the actuator. This velocity command is compared with velocity measured by the tach and appropriate correction made to the torque motor drive signal, all accomplished within the power amplifier. If the actuator length, measured by the encoder, is

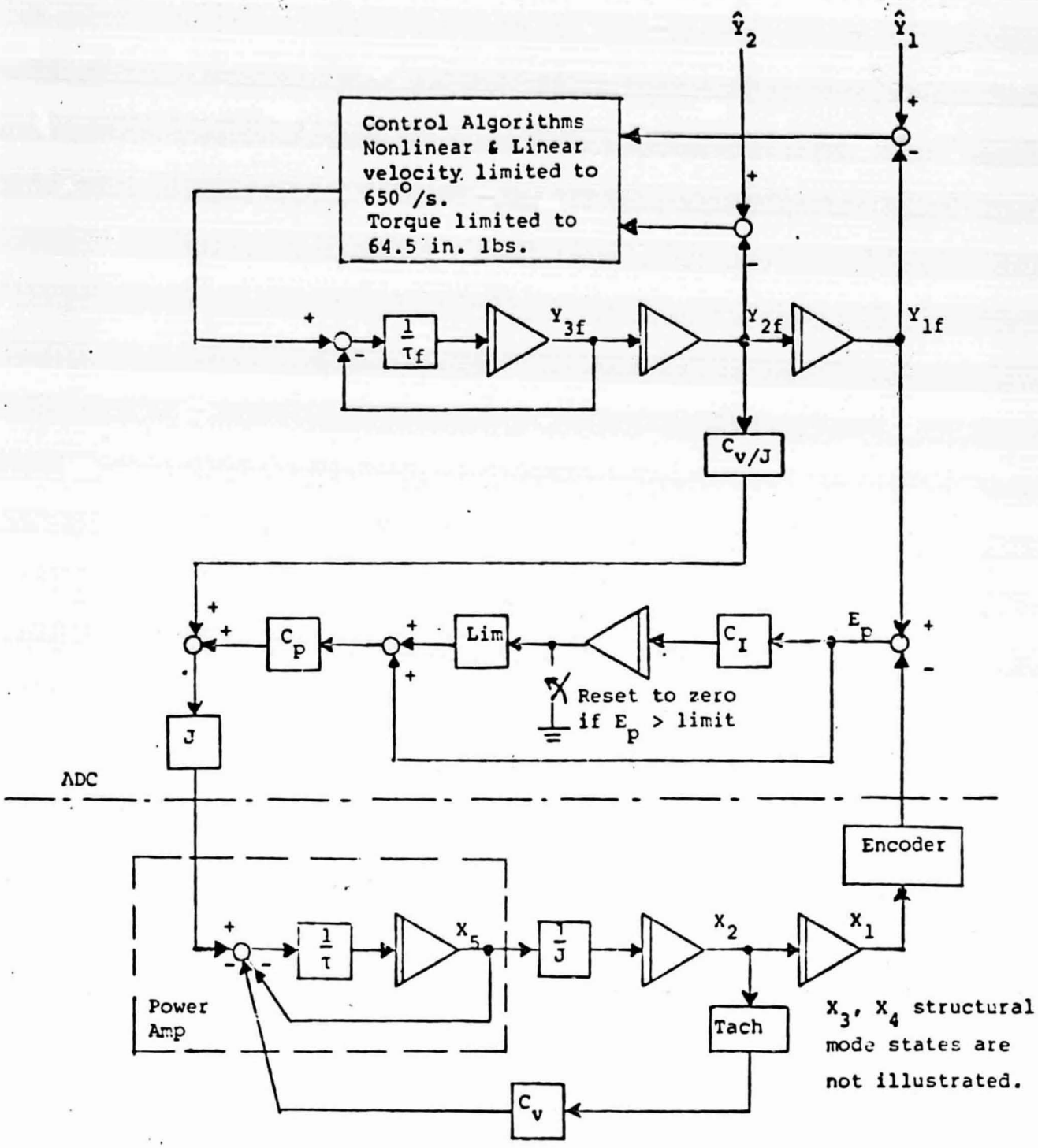

FIGURE 2.1-6: Actuator Loop Control Approach Using Tach Feedback

different from the desired length this difference is fed forward through the gain C_p to adjust the torque and minimize the error in actuator length. The error is also fed through C_I and integrated to provide additional correction to bring the difference in angle to zero. Results achieved with this loop, both in the computer simulation and on actual hardware, are provided in Section 3.

2.2 HARDWARE DESCRIPTION

2.2.1 DIGITIAL CONTROLLER DESCRIPTION

2.2.1.1 INTRODUCTION

A detailed description of the All Digital Controller is provided in Appendix A. There the system is described for general applications and its many features are described in detail. The purpose of this section is to 1) discuss requirements for the Solar Optical Telescope application for the All Digital Controller, 2) discuss improvements made to the All Digital Controller for the SOT application, and 3) define differences between the unit described in Appendix A and the unit recommended for SOT and/or the system presently owned by NASA for use on SOT.

2.2.1.2 DIGITAL CONTROLLER PROCESSOR UNIT

2.2.1.2.1 PROGRAM MEMORY EXPANSION

Control of the Solar Optical Telescope Articulated Primary Mirror requires additional capability over what had been originally designed into the All Digital Controller. In particular, it requires an increase in the size of program memory, originally 1K. This had proved adequate for the seven SIPS Loops, for which the Digital Controller was originally designed, and the two axis, but very complex, control for NASA's SGRS System. The digital controller instruction set is quite efficient in use of program memory as illustrated by the fact that the multiple transformations and algorithms for six control loops is

still contained in a program memory approximately 1K in size. However, to meet the SOT requirement program memory was expanded to 4K. Program memory word size was increased from 16 bits to 18 bits to enable direct branching within this 4K memory. While expanding directly to 4K memory, a capability was included for expanding further to 65K, if the need arises. For large program memory applications, program memory is broken down into 4K pages as described in Appendix A.

2.2.1.2.2 DATA MEMORY REFERENCED BRANCHING

To enable the program to jump to new areas in program memory, a capability to perform data memory reference branches was provided. Data memory is 16 bits wide, so that branching over the entire 65K program memory is possible. Since data memory can be accessed externally during operation, different branching locations can be commanded externally and the functions which the loops are performing controlled in this manner. This approach eliminated the need for "function memory" previously used for providing external control over the functions the digital controller was performing. This in turn eliminated some circuitry in this one area. The new commands make the system much more flexible in its overall application.

The capability for loading constants directly from program memory into the accumulator is now provided. This change was a natural fall out of the change that provided data referenced branching for the program.

2.2.1.2.3 DATA MEMORY EXPANSION

Although data used in the present SOT program does not overflow the 1K of data memory allotment of the All Digital Controller other functions such as monitoring and/or control of the alignment sensors would create an overflow. Therefore, the size of data memory was also increased, from 1K to 2K at the time the modification was made to increase the size of the program memory. Although only 2K is presently available, the SOT system will be able to access directly 4K of data memory. All that is required is adding the memory. Although the mechanization is not complete, indirect access to as much as 65K of data memory is planned for.

2.2.1.2.4 INDEXING CHANGE

Prior to the increase in memory size, as part of the effort to squeeze the SOT program and data into the existing memory sizes, the efficiency of the All Digital Controller in use of memory, especially data memory, was improved by modification of the indexer circuitry. The indexer circuitry provides the All Digital Controller with the capability of using a single program for control of all 6 extendable links. It is one of the features that makes the Digital Controller so efficient in program use in handling multi-axis control configurations. The first of two changes involved loading the indexer from the accumulator rather than program memory. This allows easy control of multiple loop configurations. In a second

change, selection of the direct or indexing mode of accessing data memory is now accomplished by examining the last 3 bits of the data address. If these are all zeros an indexing mode is assumed. This approach allows all data related functions of the All Digital Controller to be accomplished in either the direct or indexed mode. For the SOT system this greatly facilitated the use of a single set of constants for all 6 loops and saves considerable data memory.

2.2.1.2.5 ALU-ACCUMULATOR MODIFICATION

In reaccessing the system's conversion to one suitable for a space mission, it was discovered that problems had occurred in processing the 54S281J IC which made it questionable for qualification as a high reliability part. This IC was used as the accumulator for the All Digital Controller performing all the basic arithmetic functions. It was suggested to NASA that in making the memory expansion it would be a convenient time to convert to a new ALU chip. A change was made to use the 2901, an ALU chip which has gained widespread usage and is available in 883B and other high-rel configurations. Use of the 2901 results in less chips in the system and provides a minor savings in power. Addition of the 2901 removed the only known areas at present where a qualification problem could occur for the All Digital Controller.

2.2.1.2.6 INDIRECT ADDRESSING AND MEMORY 2

These two changes were added in response to another application and were not paid for using NASA funds. However, the capability is included in the NASA system intended for SOT. The indirect addressing capability comes about from a register which accepts addresses computed in the arithmetic logic unit (ALU). Data memory or Memory 2 can then be accessed using this computed address and the data loaded into the accumulator. This provides the capability for constructing and using non-linear tables.

The Memory 2 modification provides for accessing an additional 4K of data memory, directly without resorting to paging techniques. However, only loading and storing between the accumulator and Memory 2 are permitted, although this may be either directly or indirectly as commanded. No additional data memory is provided for the SOT system beyond the 2K previously discussed. However, to facilitate checkout, 1K of that 2K is jumper selectable to be either main Data Memory or Memory 2. In the "other" application, which sponsored these changes, 4K of Memory 2 is provided on PROM's for use as "look up" tables.

2.2.1.2.7 PRINTED CIRCUIT BOARD MECHANIZATION

The digital controller previously was implemented on wire wrap boards, Navtrol took advantage of the opportunity to sell several systems to convert the system to use printed circuit boards.

In making the change to printed circuit boards the 5 volt regulators on each of the boards was eliminated so that now a single 5 volt regulator provides power to all three boards of the processor unit. Locating the 5 volt regulator off the board simplifies the problem of removing heat from the system. It also allows the system to be operated from a remote 5 volt supply, should that be required.

2.2.2. MOTOR - ENCODER INTERFACES

The Solar Optical Telescope program at Navtrol included the design, development and construction of motor-encoder interfaces applicable to control of the 6 SOT actuators. These interfaces communicate with the Digital Controller Processor Unit over 4 differential lines with data transferred at a rate of 2 MHz. The communication portion of this interface is described in detail in Appendix A. Only the functions unique to SOT will be described in the following paragraphs.

2.2.2.1 ENCODER INTERFACE

The encoder selected for use on the SOT APM breadboard system is a Baldwin 5Vn278Z incremental encoder. Characteristics of this encoder are described in Section 2.2.3. The encoder has three sets of push pull output lines, one set each for sine wave, cosine wave, and index pulse. The encoder has 4096 lines resulting in 4096 psuedo-sine and cosine waves per revolution. As received from Baldwin, the encoder included no electronics other then the incandescent light

source and the photo cells. Navtrol has constructed a circuit board which fits inside the encoder case which provides amplification for the sine and cosine signals and detection of the index pulse.

The amplified sine and cosine signals and the TTL compatible index pulse are passed on to the encoder interface. The amplification enbables the signals to be sent to the interface at a high enough level to minimize interference problems. Adjustments are included within the encoder to equalize amplitude of the $\pm$ swings of the signals and to provide proper overall amplitude adjustment. The zero cross over is separately adjusted so that time above and below the zero level is also equalized.

Figure 2.2-1 is a functional block diagram for the encoder interface. The interface provides a times 16 multiplication of the basic sine and cosine signals from the encoder. That is, each cycle, represented by a line on the encoder disk, will be subdivided into 16 parts. This is equivalent to adding 4 bits to the basic 12 bit accuracy provided by the encoder. Pulses are derived only for the sine wave crossings and counted. The additional interpolation is all done logicially so as to minimize the possibility of dropped pulses. The basic 2^{12} resolution, provided by the encoder disk lines, is approximately sufficient for $.1^{o}$ accuracy at the actuator. As shown in Section 3, the sensitivity of the system is such that if each of the actuators contributed $.1^{o}$ error rms the result at the mirror would be approximately .6 arc seconds rms. This

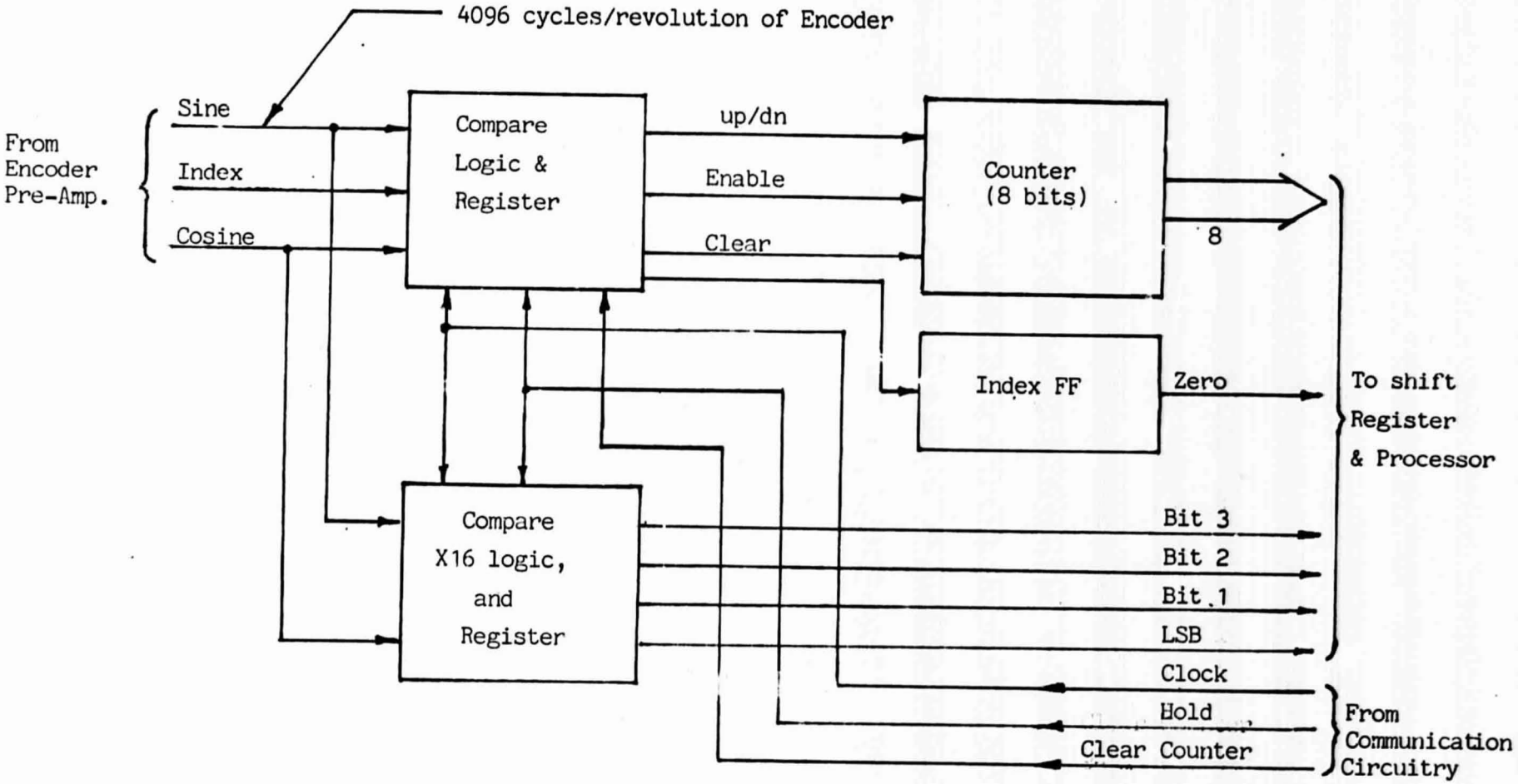

FIGURE 2.2-1 Encoder I/F Block Diagram
(Provides 16 bit resolution)

sensitivity is 4 to 6 times greater than originally anticipated, and higher resolution on the encoder might be desirable. However, the additional times 16 multiplication provides sufficient resolution that it should be possible to meet the .1 arc second accuracy required. Note that resolution does not imply accuracy and 16 bit accuracy may not be achieved. Navtrol now feels that an encoder with 2^{14} lines would provide greater assurance that the final system accuracy requirements would be met.

Referring back to Figure 2.2-1, the box labeled "Compare, Logic and Register" senses when the sine wave changes sign at the same time that the cosine wave is high, and puts out an appropriate up or down pulse to the counter signifying a line crossing. If, at the same time that a line crossing occurrs an index pulse is received the counter is cleared and the index flip flop set. This signifies to the computer that the zero reference line of the encoder was crossed during the last sampling interval. The angle of rotation which has occurred since the index was actually received will be indicated by the count within the counter and the logical interpolation signals.

The counter is also cleared each time it is read out to the IO shift register. Therefore the counter reading represents the angle rotated through during 1 sample period, except when an index pulse is received. Then, the

counter reading is absolute. The sampling rate, 256 times per second, is such that an overflow of the counter cannot occur within the rates that will be encountered in system usage.

The remaining block on the diagram performs the times 16 logic function and stores the result in a register. These additional 4 bits are loaded into the IO shift register at the same time as the counter outputs and are transferred as one word. However, they represent the 4 least significant bits of the measured absolute angle, not the difference angle. This is taken into account in the processor program.

The counter is cleared synchronously with the load into the IO shift register. To insure that a pulse is not fed to the counter at the same time as the clear signal a "hold signal" is issued from the IO which holds any pulses in the register until after the counter is cleared. This insures that no pulses will be dropped due to this circumstance.

The reason for Navtrol designing the circuitry, rather than buying the circuitry from Baldwin Electronics, is that Baldwin does not offer a times 16 multiplication for this encoder. Their attitude is that resolution implies accuracy. Since they do not want to guarantee 16 bit accuracy from this encoder, they do not offer the times 16 multiplication of the basic number of lines from the

the encoder. However, in control applications for smoothness of control it is best to have additional bits even though the angle, when referred back to the index position, may not be accurate to the resolution increment. In addition, if the times 16 multiplication was done inside the encoder the number of pulses occurring per cycle would be 16 times that used in the Navtrol implementation. Distortion in the sine wave could result in a dropped pulse and in this latter implementation this pulse would not be recovered until the index line is again crossed. By performing the times 16 multiplication with hard logic Navtrol assures that dropped pulses will not occur.

In addition to receiving and performing functions on the signal as just described, the encoder interface also supplies $\pm$ 15 volts to the pre-amp and 5 volts for the illuminator lamp within the encoder.

2.2.2.2 MOTOR DRIVE AMPLIFIER

The torque motor which the Motor Drive Amplifier must drive is a brushless DC motor with the 3 phases in the armature connected in delta. The inductance and resistance between two terminals of the motor are 15 mh and 3.15 ohms respectively, providing a motor electrical time constant of approximately 5 milli-seconds. With 28 volts applied the maximum current will equal approximately 8 amps. The motor provides a torque of 125 oz. in. per amp. Additional information on this motor is provided in

in Section 2.3.

The functional diagram for the motor drive amplifier is provided by Figure 2.2-2. The amplifier is a pulse width modulated amplifier so that the output current switches on the right hand side of the diagram are either on or off. This greatly reduces the power required overall but especially within the power amplifier itself. This in turn greatly eases the problem of cooling the unit. For example the running friction in each actuator is expected to run as high as 8 in. lb. To overcome this friction requires current in access of 1 amp. If a linear output amplifier were used this would result in a continuous power requirement of 28 watts, with 25 watts used in the output stages of the amplifier. For the Navtrol pulse width modulator amplifier the power to the motor remains the same, of course, but the continuous power in the output amplifier, is less than 2 watts, so that the total power is approximately 3.5 watts. Again, this is only the DC power in the output circuitry not the total module power. A small amount of switching power in the output stages is also used.

Referring again to Figure 2.2-2, the data received through the IO from the Digital Processor unit is held in a 16 bit register. Of the 16 bits, 12 bits represents the magnitude of the velocity command, one bit defines sign and the other 3 bits define the commutation angle for the

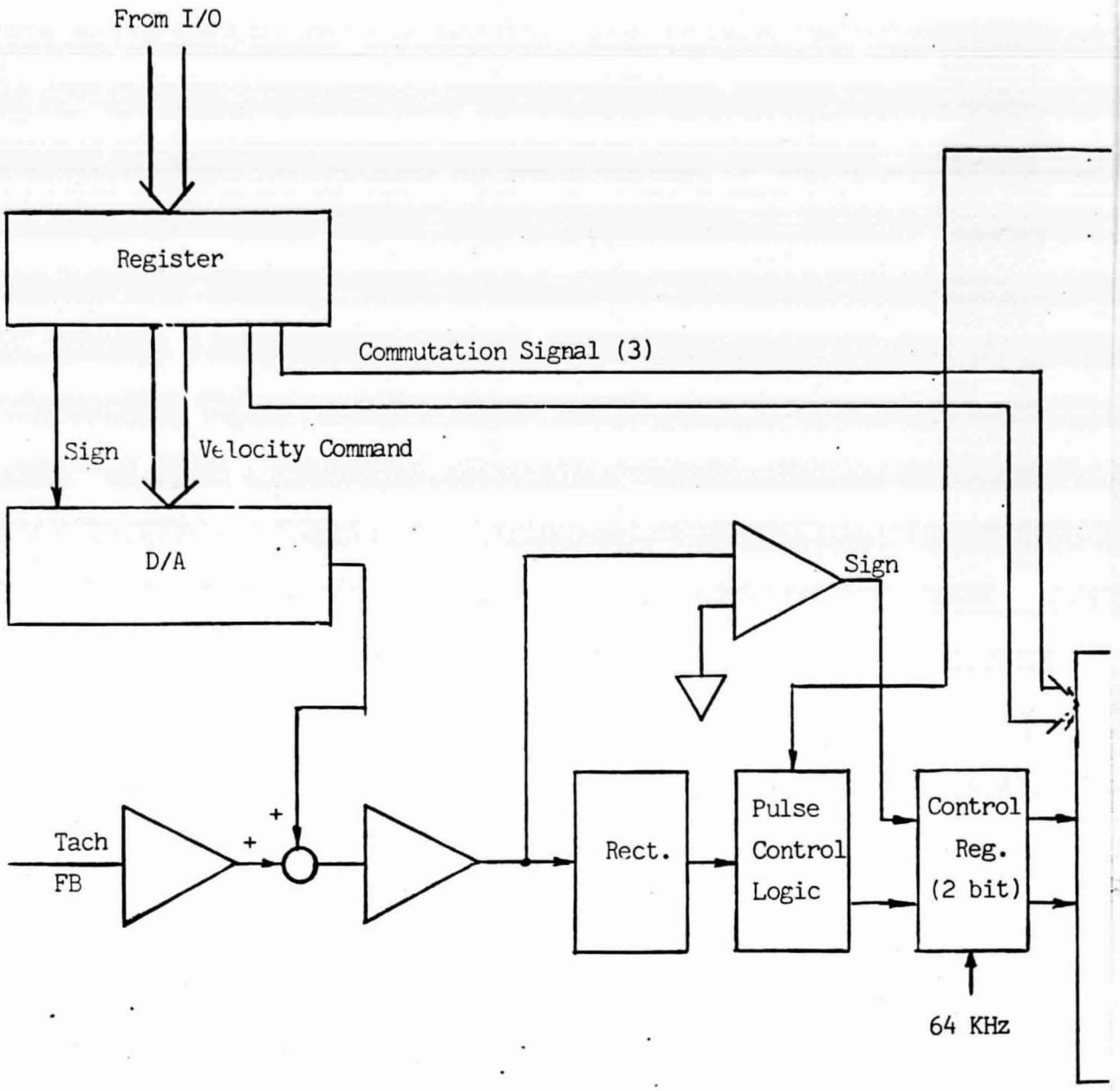

FIGURE 2.2-2: Motor Drive Amplifier Functional Block Diagram

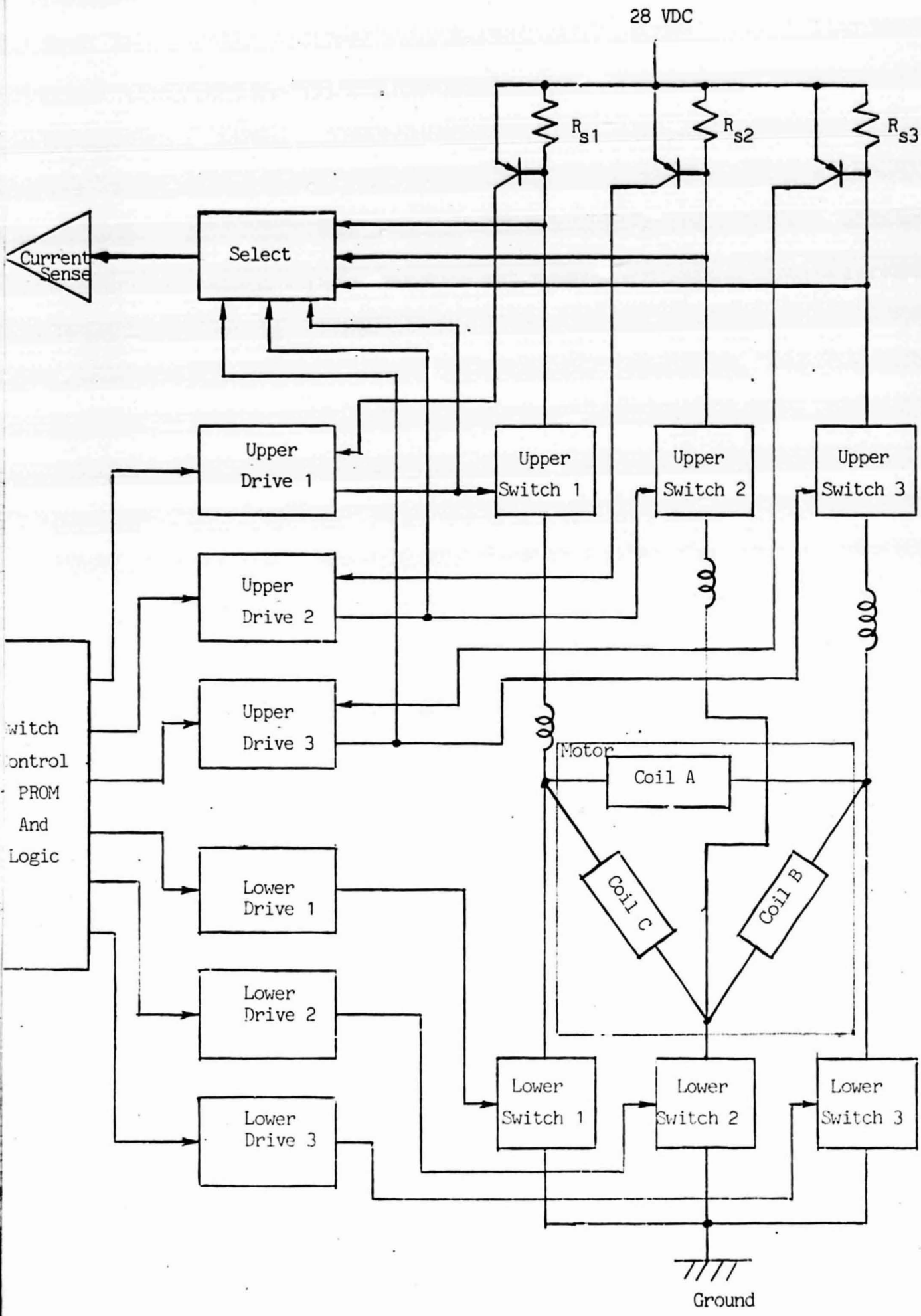
28 VDC
R_{s1}
R_{s2}
R_{s3}
Current Sense
Select
Upper Drive 1
Upper Drive 2
Upper Drive 3
Upper Switch 1
Upper Switch 2
Upper Switch 3
witch
ontrol
PROM
And
Logic
Motor
Coil A
Coil B
Coil C
Lower Drive 1
Lower Drive 2
Lower Drive 3
Lower Switch 1
Lower Switch 2
Lower Switch 3
Ground

brushless motor. Providing commutation based on encoder measured angles provides the most accurate method for performing this function. The output of the D/A, the velocity command, is compared to the tach feedback signal and the difference amplified. The sign of this signal controls the sign of the torque motor current. The magnitude of the signal defines the pulse width of voltage applied across the motor coil. The pulse is kept on until the motor current, fed back through the current sense amplifier, equals the magnitude commanded. The output on-off command, along with the sign, is sampled and held 64,000 times per second. The sampled information is passed through the "switch control logic " to control the appropriate upper and lower switches, providing torque in proper direction.

In the Navtrol design, the upper switches remain turned on during the entire sampling interval while the lower switch is turned on and off to adjust to the proper output current level. The design is such that the output current through the motor coil always flows through the appropriate sense resistor, R_{s1}, R_{s2} or R_{s3}, selected by the upper switch. The output current is measured to an accuracy of approximately 1%. This is made equal to commanded current for accurate control of commanded torque, which is directly proportional to output current.

Across each sense resistor is a transistor which

turns on if the sense resistor voltage exceeds a level indicating excessive current. This, in turn, cuts off the appropriate upper switch. For example, if a motor coil is momentarily grounded, the amplifier is designed to cut off before damage to the upper switch can occur. The coils in series with the motor provide sufficient time for the cut off to occur before excessive current is drawn.

The output power stages are designed to minimize voltage drop and power loss. The sense resistors are only .05 ohms and the nominal value of resistance for both the upper and lower switches is .055 ohms each. The resistance of the series coil is approximately .01 ohms providing a total resistance in series with the motor coils of only .17 ohms. It is this very low resistance that insures a low power dissipation in the output stages of the motor drive amplifier.

Another feature of the design is that whenever sign changes all switches are momentarily (500 ns) turned off before a new set of switches, upper and lower, are selected. This insures that the switches that are to be turned off are off before a new set is turned on, reducing transients in the system and strain on the output transistors.

Figure 2.2-3 illustrates the gain distribution in the Motor Drive Amplifier corresponding to velocity loop bandwidth of 400 Hz.

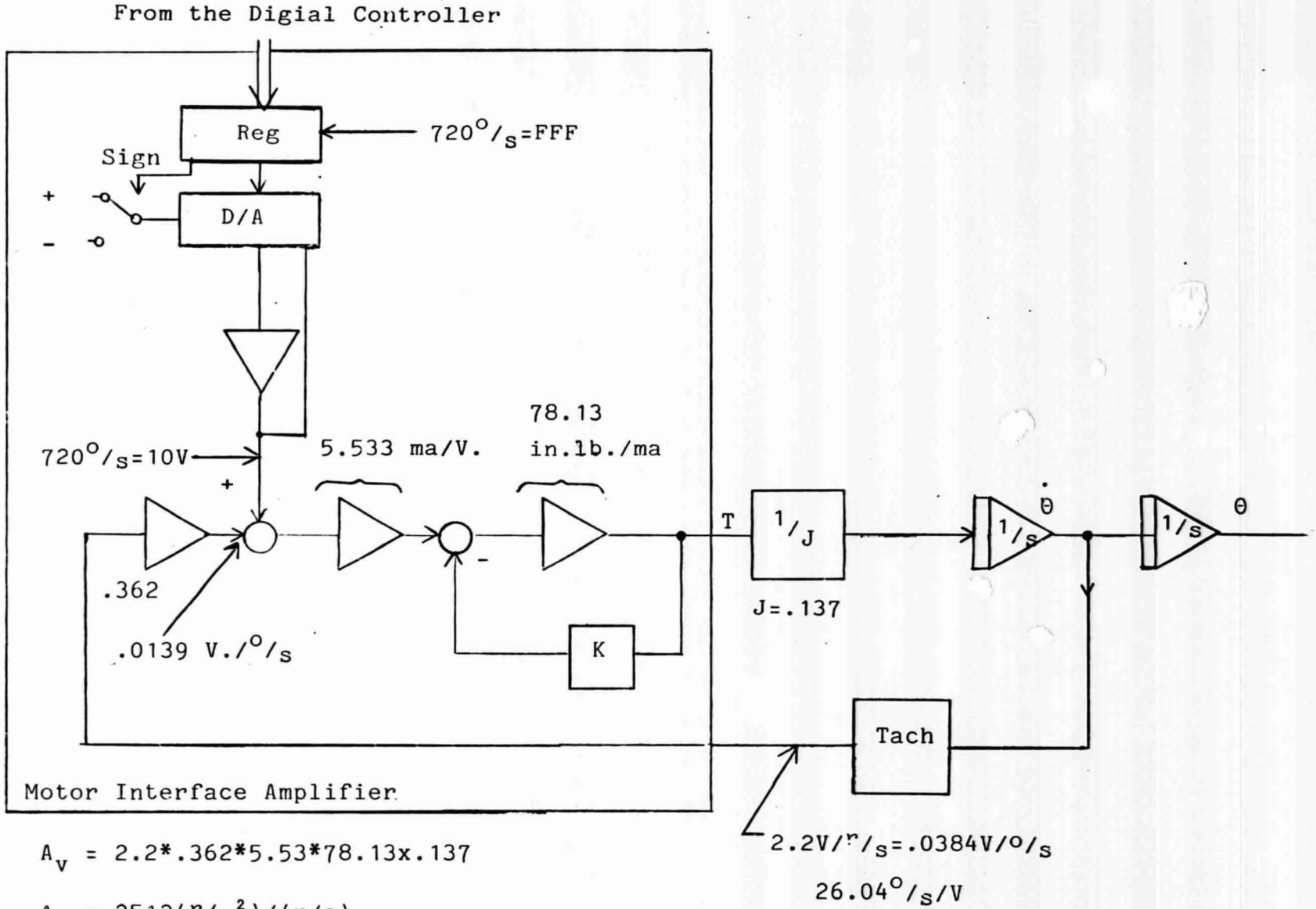

$A_v = 2.2*.362*5.53*78.13x.137$

$A_v = 2512(r/s^2)/(r/s)$

$f_v = A_v/2\pi = 400$ Hz

FIGURE 2.2-3: SOT POWER AMPLIFIER
2/4/80 RJB

2.2.3 ACTUATOR CONTROL

Figure 2.2-4 is a photograph of the SOT APM actuator assembly provided through courtesy of Sacramento Peak Observatory, where the assembly was constructed under direction of Dr. Dick Dunn. The assembly contains a fly-wheel (19 times motor inertia), which may be removed if required, a motor, a tachometer and an encoder. The length of the actuator itself, including the encoder, is 18 inches, and the largest diameter, around the inertia wheel, is 7.75 inches. A small linear displacement sensor is located beside the assembly toward the viewer.

Friction was measured at 4.5 in. lb.. Measurements of backlash were also made and a plot is provided in Section.3. Both of these measurements were made at Sacremento Peak Observatory.

The characteristics of the torque motor included in the actuator are described on Table 2.2-1.. The characteristics of the SOT APM tachometer are given on Table 2.2-2. The encoder is a Baldwin series 5VN278 manufactured by BEI Electronics, Inc, Little Rock, Arkansas. It is a incremental encoder with 4096 lines per revolution. It uses an incandescent lamp as the light source, which may not be desirable in a space environment. However, similar encoders are available with LED illumination. Outputs from the encoder are 3 sets of push pull signals derived from 6 internal photocells, two for each of the 3 outputs.

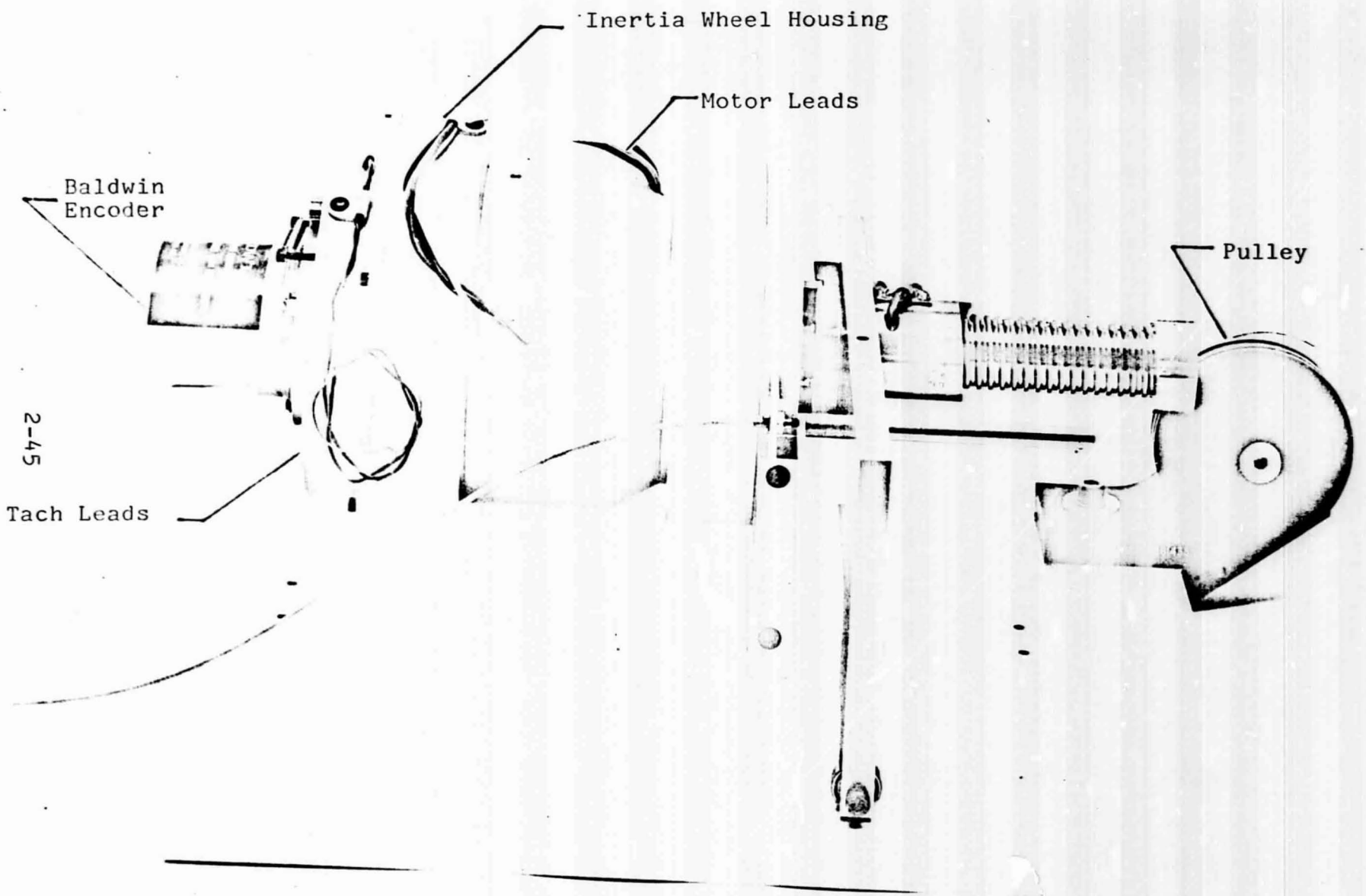

FIGURE 2.2-4: SOT APM Actuator Assembly

TITLE BM-3203 [illegible]

WRITTEN BY: M. Fleisher DATE [illegible]

APPROVED BY: [illegible] DATE [illegible]

ISSUE: 1

SHEET NO. 1 OF 1

MACHINE TYPE

Synchronous motor having 8 poles in a permanent magnet field, and three phases in the armature connected in delta with three terminals for operation as a brushless d-c motor.

SIZE CONSTANTS

Peak torque - T_p	1250	oz-in
Torque per square root of power - K_M	70.7	oz-in/$\sqrt{W}$
Power input, stalled at T_p (25°C) - P_p	313	watts
Static friction - T_F	18	oz-in
Maximum allowed winding temperature	155	°C
Temperature rise per watt - TPR' (when mounted)	0.6	°C/W
Rotor inertia - J_M	.160	oz-in-s^2
Motor weight	120	#

WINDING CONSTANTS

JUL 31 1979 B

Winding designation		
Voltage between two terminals at maximum current, stalled and 25°C - V	31.5	volts
Maximum allowed line current - I	10.0	amperes
Resistance between two terminals at 25°C - R ± 12-1/2%	3.15	ohms
Torque per unit line current - K_T ± 10%	125	oz-in/A
Back EMF between two terminals per unit speed - K_B ± 10%	0.883	V-s/rad
Inductance between two terminals - L ± 30%	15	mH

ORIGINAL PAGE IS OF POOR QUALITY

TABLE 2.2-1 : SOT APM Torque Motor

Model No. TG-2936			
Max. Sensitivity Volts/Rad/Sec			2.20 *
Tach Generator Friction Torque lb-ft			.014
Ripple Voltage, Peak to Peak %			1.0
Ripple Cycles per Revolution			91
Rotor Moment of Inertia lb-ft-Sec^2			2.1×10^{-4}
Tach Generator Weight Ounces			24
Max. Permissible Winding Temp. ^{o}C			105
Max. Terminal Voltage (Volts)			150
Max. Speed due to Brushes (Rad/Sec)			90
*Special Winding			
Winding Designation		A	C
DC Resistance Ohms @ 25^{o}C	±12½%		1230
Volts Sensitivity Volts/Rad/Sec	±10%		2.20
Inductance Henrys	±30%		1.1
Min. Load Resistance Ohms			120K
Max. Operating Speed Rad/Sec			68
Volts @ Max. Operating Speed			150

(6) ECN-43383 WAF 3-30-77
(5) ECN-42923 WAF 9-27-76
(4) ECN-32464 7-12-71 RL
(3) ECN-32272 6-21-71
(2) ECN-31580 4-26-71 BCS
Checked By R.W. Date 3-4-71
By B.C.S. Date 2-24-71 Subject TACHOMETER CATALOG DATA SHEET
Issue 7
Sheet No. 1 of 1

TABLE 2.2-2 : SOT APM Tachometer

As delivered from BEI, no electronics are included as these are part of the Navtrol interface circuitry. Specifications for this encoder are included in the Appendix B of this report.

The motor, encoder, and tachometer were selected for use in a mock up system and may not represent the appropriate choice for a space fight environment. Availability played a large part in the initial selection process.

2.2.4 SERVO DEVELOPMENT SYSTEM

Navtrol has developed a graphics capability to be added to their previous Software Development System to permit recording of data available only in digital form within the All Digital Controller. This includes not only a CRT but a printer as well to preserve servo responses and other system plots obtained during tests. This capability was developed using Navtrol R & D funds to overcome problems encountered in the past in accessing error signals, output commands and angular measurements from the encoder and other devices, available only in digital form and buried deep inside the All Digital Controller. This graphics capability is new and is not presently a part of the NASA system planned for use on the SOT mock up.

3.1 ANALYSIS AND SIMULATION RESULTS

3.1.1 TRANSFORMATION RESULTS

3.1.1.1 PRECISION TRANSFORMATION

Section 2.1 of this report provides definition of the overall control approach. Section 2.1.3 discusses the transformation and provides the equations both for the actual transformation and the approximation that Navtrol uses in its Digital Controller, referred to as the "Precision" transformation. Table 3.1-1 provides a comparison of the "precision" transformation with the actual transformation. The actual transformation results were obtained on a CDC Cyber 72 computer so that truncation and round-off is negligible. The precision transformation results were obtained from the All Digital Controller. The two sets of results were subtracted point by point with the results of this computation presented on Table 3.1-1. As indicated by the Table, the errors in the All Digital Controller are negligible except for large angular rotations (.5 deg.). These errors come about because of the algorithms used rather than truncation and round off errors in the computer. By use of additional terms in the series approximation of the sine and cosine these errors could be reduced to be negligible also. This point is demonstrated on the table

TABLE 3.1-1

"Precision" Transformation Results

A. Result of Commanded Offsets.

ADC

	ΔX = 3cm	ΔY = 3cm	ΔZ = 1cm	$\theta x = .1^{\circ}$
ΔX(cm)	-8.1×10^{-8}	-4.6×10^{-7}	-4.7×10^{-7}	-2.0×10^{-7}
ΔY(cm)	-1.7×10^{-21}	-2.8×10^{-7}	0.0	9.6×10^{-8}
ΔZ(cm)	-4.0×10^{-8}	-6.9×10^{-9}	-8.6×10^{-8}	-1.4×10^{-7}
$\Delta\theta x(\widehat{sec})$	6.8×10^{-18}	1.5×10^{-4}	-1.4×10^{-18}	-2.3×10^{-4}
$\Delta\theta y(\widehat{sec})$	-6.5×10^{-5}	-2.0×10^{-4}	-2.7×10^{-5}	-8.8×10^{-5}
$\Delta\theta z(\widehat{sec})$	1.0×10^{-18}	6.1×10^{-4}	-3.4×10^{-19}	-6.8×10^{-5}

	ADC $\theta x = .5^{\circ}$	ADC $\theta x = .5$ $\theta y = .5$	Theoretical $\theta x = .5$ $\theta y = .5$
ΔX	-2.2×10^{-5}	2.2×10^{-4}	2.2×10^{-4}
ΔY	-1.2×10^{-6}	2.5×10^{-4}	2.5×10^{-4}
ΔZ	-1.5×10^{-6}	2.6×10^{-6}	2.9×10^{-6}
$\Delta\theta x$	-2.3×10^{-2}	-1.4×10^{-1}	-1.4×10^{-1}
$\Delta\theta y$	-9.7×10^{-3}	-7.7×10^{-4}	-1.3×10^{-3}
$\Delta\theta z$	9.5×10^{-4}	-1.1×10^{-3}	-8.2×10^{-4}

These are "open loop" results. The sensors shuld detect these errors and reduce them further.

by comparison of the ADC results with $\theta_x = .5$ and $\theta_x = .5$ with the theoretical results obtained at the same offset angles. The "theoretical" result was obtained on the CDC computer using the same algorithms as used in the All Digital Controller.

These transformation results are all open loop and will be reduced further by the sensors detecting any errors and feeding them back into the closed loop system. Navtrol's specification for open loop results was 1 arc second which the algorithms meet by a wide margin. It is apparent that if the sensors can measure the small errors, closed loop action should be able to remove most of the remaining error. The conclusion is that the "precision" transformation, as programmed in the All Digital Controller is sufficiently accurate to provide the accuracy required in control of the Articulated Primary Mirror of the Solar Optical Telescope.

3.1.1.2 "FAST" TRANSFORMATION

The so called "fast" transformation is utilized in the All Digital Controller for transforming rates from each of the sensors to each of the links. The rate transformation is updated 64 times per second, and at the time of update is essentially correct. Theoretically, the rate transformation is correct at the precise set of conditions to which it applies. The high update rate keeps the rate transformation accurate as the mirror is moving.

Prior to the program at Navtrol it was suggested that it might be possible to use a constant transformation. Although closed loop nulling of the system may be sufficient to eventually bring the mirror to the null positions of the sensor, a round about route will be taken to get there resulting in extraneous motions that Navtrol believes could not be tolerated.

Table 3.1-2 illustrates the differences between a transformation at the neutral position of the mirror and at an offset position. The differences in the two matrices are obvious with many terms exhibiting not only considerable variation in magnitude but even changes in sign. Navtrol believes that the smooth transformation of rate will allow smooth control without extraneous motion that could decrease accuracy especially dynamic accuracy. Note that the last column of the transformation matrix is not required since θ_z, roll, is always assumed to be zero. The accurate transformation minimizes the possibility that this would not be so.

To test out the accuracy of the fast transformation for transforming rate a series of runs were made in which an offset and a rate were commanded for one sensor at a time in turn for each of the sensors, except for the last run which included simultaneous offsets and rates in two sensors. The resulting rate at each actuator linkage was recorded. This rate was compared to the position change calculated

TABLE 3.1-2: "FAST" Transformation

A. Zero Position Matrix; $\Delta x = \Delta y = \Delta z = 0.0$; $\theta_x = \theta_y = \theta_z = 0.0$

.19827488	-.73996399	-.64275996	-336.55468	-57.457118	-37.672137
.19827488	.73996399	-.64275996	336.55468	-57.457118	37.672137
.54173769	.54167102	-.64273850	218.02745	-262.75903	-37.675148
-.73998437	-.19832914	-.64271976	-118.54424	320.20489	37.675704
-.73998437	.19832914	-.64271976	118.54424	320.20489	-37.675704
.54173769	-.54167102	-.64273850	-218.02745	-262.75903	37.675148

B. Offset Position Matrix; $\Delta x = \Delta y = \Delta z = 0.0$; $\theta_x = \theta_y = .5^\circ$; $\theta_z = 0.0^\circ$

-.093254342	-.55388893	-.82735160	-239.88408	95.060886	-36.602263
-.064304058	.83523368	-.54612242	386.12362	64.081259	52.540435
.25188479	.77834177	-.57509837	337.52389	-122.17168	-17.517328
-.86134755	.066349096	-.50366477	14.667870	387.44468	25.954704
-.78743137	.36781077	-.49463833	195.59882	352.13676	-49.533070
.34328709	-.34301233	-.87435491	-105.56426	-166.50454	23.873901

$$\begin{bmatrix} \Delta L_1 \\ \Delta L_2 \\ \Delta L_3 \\ \Delta L_4 \\ \Delta L_5 \\ \Delta L_6 \end{bmatrix} = \begin{bmatrix} \text{Fast Tranformation Matrix} \end{bmatrix} \cdot \begin{bmatrix} \Delta X \\ \Delta Y \\ \Delta Z \\ \theta_x \\ \theta_y \\ \theta_z \end{bmatrix}$$

Linear dimensions are in centimeters. Angles are in radians.

for the same set of conditions, using the actual transformation on a CDC Cyber computer. The difference in position divided by the time over which the positional samples were taken provides an accurate measure of the "average" rate over the sample. By averaging the link rates obtained by use of the rate transformation, a direct comparison was made. Table 3.1-3 presents the results of those test runs. It is divided into two sections, the upper section defines both the conditions of each of the sensors (the input conditions) and the resultant rates of each of the links. The measured error for each of the six conditions and for each of the 6 links is provided in the lower section of the Table. Navtrol believes these indicate sufficient accuracy of the rate transformation that smooth control can be achieved. The results could be improved by use of double precision and/or a higher update rate but this does not appear to be needed. Bear in mind that the results above were obtained with the input rates set at the maximum rates expected. Lower rates should improve results but were not run. This should probably be accomplished.

3.1.1.3 ERROR SENSITIVITY ANALYSIS

By inverting the matrices of Table 3.1-2 the sensitivity matrices shown on Table 3.1-4 are obtained. These matrices define the sensitivity, about a given set of conditions of the sensor measured parameters to errors in controlling

RUN CONDITION

Except as indicated $\Delta S_i=0$, and $\dot{S}_i=0$ for each of the runs.

Run No.	1	2	3	4	5	6
Link No.	Δx=3cm $\dot{x}$=0.1cm /sec	Δy=3cm $\dot{y}$=0.1 cm /sec	Δz=3cm $\dot{z}$=0.1cm /sec	$\Delta\theta_x=2.5^0$ $\dot{\theta}_x=63\frac{sec}{sec}$	$\Delta\theta_y=0.5^0$ $\dot{\theta}_y=63\frac{sec}{sec}$	$\Delta\theta_x=0.5^0$ $\Delta\theta_y=0.5^0$ $\dot{\theta}_x=\dot{\theta}_y=63$ sec/sec
1	26.7	57.6	-35.4	84.1	17.0	97.6
2	46.9	46.9	-35.4	66.5	-31.6	46.7
3	-44.4	-147	-35.4	37.1	81.9	87.2
4	-44.4	26.7	-35.4	49.8	81.9	118
5	46.9	-26.7	-35.4	-19.3	-31.6	-58.7
6	26.7	-44.3	-35.4	-52.7	17.0	-31.3

The tabulated results are link velocities in degrees/second

Resultant Link Velocity Error in degrees/seconds

Run # / Link #	1	2	3	4	5	6
1	0.0175	0.0122	0.0145	0.039	0.0144	0.115
2	0.0094	0.0096	0.0131	0.0346	0.0255	0.015
3	0.008	0.0135	0.0131	0.379	0.0202	0.0045
4	0.008	0.0119	0.0131	0.0385	0.0202	-0.0428
5	0.0094	0.009	0.0131	0.341	0.0255	0.152
6	0.0175	0.0132	0.0145	0.0289	0.0144	Not Taken

TABLE 3.1-3: Rate Transformation Results

TABLE 3.1-4: Sensitivity Matrices

A. Zero Position Matrix; $\Delta x = \Delta y = \Delta z = 0.0$; $\theta_x = \theta_y = \theta_z = 0.0$

$$\begin{bmatrix}
+4.6329870 & +4.6329870 & -3.0015030 & -1.6316863 & -1.6316863 & -3.0015030 \\
+.79072029 & -.79072029 & +3.6171002 & +4.4076922 & -4.4076922 & -3.6171002 \\
-.25929846 & -.25929846 & -.25930712 & -.25931468 & -.25931468 & -.25930712 \\
-.00272895 & +.00272895 & -.00745753 & -.01018612 & +.01018612 & +.00745753 \\
+.01018623 & +.01018623 & -.00745687 & -.00272978 & -.00272978 & -.00745687 \\
-.00442404 & +.00442404 & -.00442384 & +.00442376 & -.00442376 & +.00442384
\end{bmatrix}$$

B. Offset Position Matrix; $\Delta x = \Delta y = \Delta z = 0.0$; $\theta_x = \theta_y = .5^o$; $\theta_z = 0.0^o$

$$\begin{bmatrix}
+4.342665 & +4.5251009 & -2.4902084 & -3.2652720 & -.69638231 & -3.0227960 \\
+1.4962789 & -2.3592453 & +5.2485450 & +4.5196996 & -4.7042482 & -3.3366927 \\
-.29663351 & +16945767 & -.60868725 & -.47563160 & +.17524583 & -.39365457 \\
-.00398387 & +.00628197 & -.01091454 & -.01070300 & +.01117056 & +.00687091 \\
+.00941527 & +.01008684 & -.00650007 & -.00601376 & -.00055852 & -.00715386 \\
-.00376025 & +.00536833 & -.00467096 & +.00520212 & -.00565950 & +.00348237
\end{bmatrix}$$

$$\begin{bmatrix} \Delta X \\ \Delta Y \\ \Delta Z \\ \Delta\theta_x \\ \Delta\theta_y \\ \Delta\theta_z \end{bmatrix} = \begin{bmatrix} \text{Sensitivity Matrix} \end{bmatrix} \cdot \begin{bmatrix} \Delta L_1 \\ \Delta L_2 \\ \Delta L_3 \\ \Delta L_4 \\ \Delta L_5 \\ \Delta L_6 \end{bmatrix}$$

Linear dimensions are in centimeters Angles are in radians

the length of each one of the links. For example, by letting each of the links, one at a time, have an error of .1 deg., the results of Table 3.1-5 are obtained. As indicated, an error in the length of any link results in errors in all 6 degrees of freedom of the mirror, including roll. For example, for the neutral position of the platform, if the error ΔL_1 is equal to .1 deg., θ_x will have an error of -.0794 arc seconds. If all of the lengths are held to an rms accuracy of 0.1 degree, then the rms error in θ_x would be .532 arc seconds. For the offset mirror, the result is .625 $\widehat{\text{sec}}$. This sensitivity is 3 to 5 times higher then previously considered. Part of this is due to the rmsing of errors from all links. The rest may be due to a change in configuration in the links or may be due to just taking a closer look at the transformation.

On Table 3.1-5 two positions are considered, one the neutral position of the mirror and the other at the maximum expected angular offset. It is expected that the errors at other attitudes of the mirror would be in line with the results presented but additional checks should be made to make sure that this is true. Since the computer program exists to perform this analysis, looking at other attitudes is not a large task but it has not been accomplished thus far.

The link configuration on which these results are based was presented in Table 2.1-1. Figure 3.1-1 illustrates

TABLE 3.1-5: Effect of Actuator Accuracy on Mirror Position

A. Zero Position; $\Delta X = \Delta Y = \Delta Z = 0.0$; $\theta x = \theta y = \theta z = 0.0$; ΔL_j* = 0.1 degree

	ΔL_1	ΔL_2	ΔL_3	ΔL_4	ΔL_5	ΔL_6	RSS
x(cm)	.654E-3	.654E-3	-.423E-3	-.230E-3	-.230E-3	-.424E-3	.115E-2
y(cm)	.112E-3	-.112E-3	.510E-3	.622E-3	-.622E-3	-.510E-3	.115E-2
z(cm)	-.366E-4	-.366E-4	-.366E-4	-.366E-4	-.366E-4	-.366E-4	.896E-4
θy(sec)	-.794E-1	.794E-1	-.217E0	-.296E0	.296E0	.217E0	.532E0
θy(sec)	.296E0	.296E0	-.217E0	-.795E-1	-.795E-1	-.217E0	.532E0
θz(sec)	-.129E0	.129E0	-.129E0	.129E0	-.129E0	.129E0	.315E0

B. Offset Position $\Delta X = \Delta Y = \Delta z = 0.0$; $\theta x = \theta y = 0.5$ deg; $\theta z = 0.0$; ΔL_j* = 0.1 degree

	ΔL_1	ΔL_2	ΔL_3	ΔL_4	ΔL_5	ΔL_6	RSS
X(cm)	.613E-3	.639E-3	-.351E-3	-.461E-3	-.983E-4	-.427E-3	.114E-2
Y(cm)	.211E-3	-.333E-3	.740E-3	.638E-3	-.663E-3	-.471E-3	.133E-2
Z(cm)	-.419E-4	.239E-4	-.859E-4	-.671E-4	.247E-4	-.555E-4	.134E-3
θx(sec)	-.116E0	.183E0	-.318E0	-.312E0	.325E0	.200E0	.625E0
θy(sec)	.274E0	.294E0	-.189E0	-.175E0	-.163E-1	-.208E0	.521E0
θz(sec)	-.109E0	.156E0	-.136E0	.151E0	-.165E0	.101E0	.339E0

$$\begin{bmatrix} x \\ y \\ z \\ \theta x \\ \theta y \\ \theta z \end{bmatrix} = \begin{bmatrix} \text{Sensitivity} \\ \text{Transformation} \\ \text{Matrix} \end{bmatrix} \cdot \begin{bmatrix} \Delta L_1 \\ \Delta L_2 \\ \Delta L_3 \\ \Delta L_4 \\ \Delta L_5 \\ \Delta L_6 \end{bmatrix}$$

*In 1st six columns all $\Delta L_j = 0$ except indicated link in which $\Delta L_j = 0.1^o$ of rotation of motor. The last column is the RSS of the other 6 columns and represents the total error expected if accuracy of each link is held to 0.1^o rotation.

3/10/80

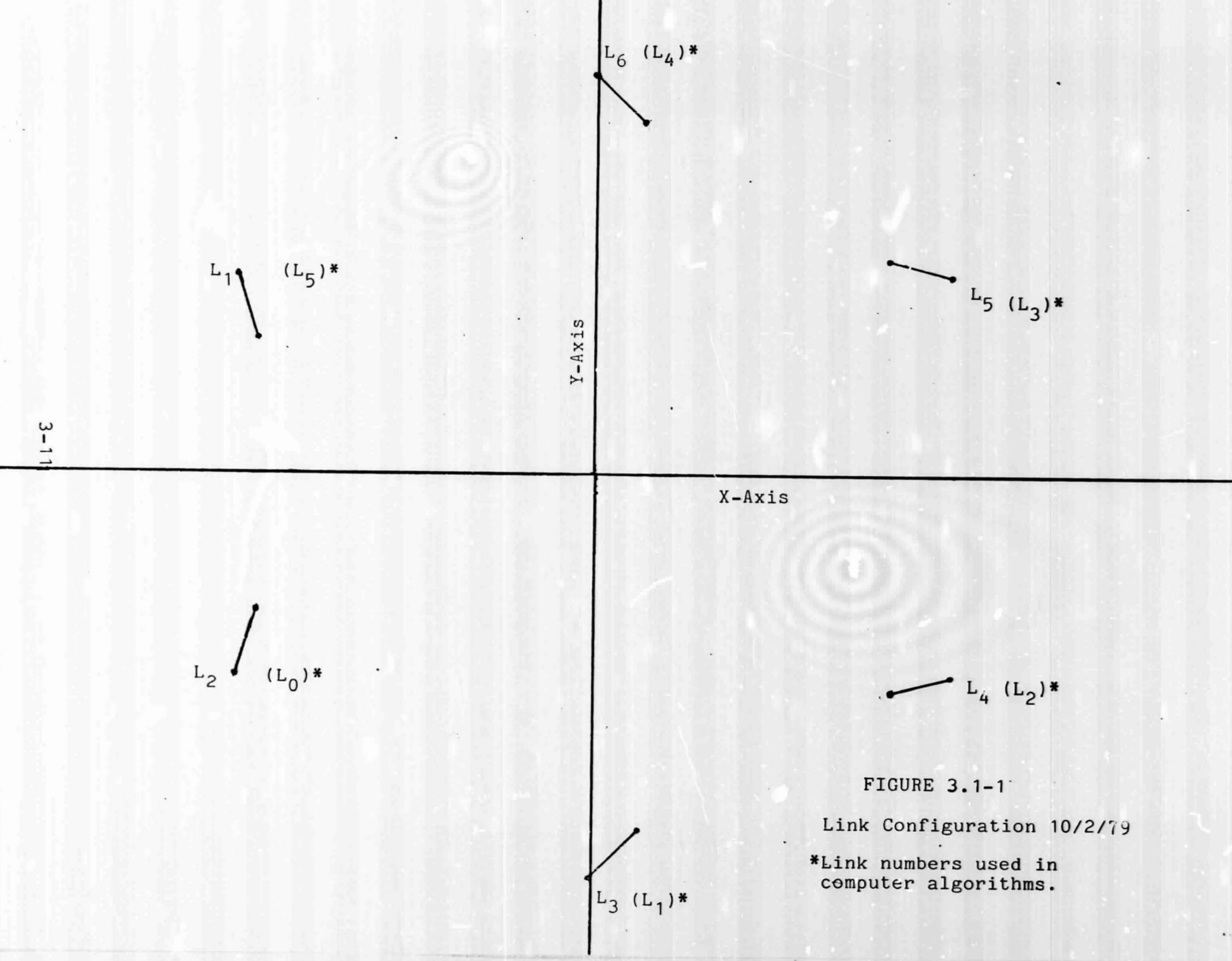

FIGURE 3.1-1

Link Configuration 10/2/79

*Link numbers used in computer algorithms.

this configuration as viewed looking down the Z axis of the coordinate system. Note that only a small amount of motion along the x axis results in a change in sign of the sensitivity for L_1 and L_2 to motion along this same axis. Likewise, a small amount of motion in the y axis results in a change in sign of the sensitivity of L_4 and L_5 for motion along the Y axis.

The link numbers in parentheses, are link numbers used in the algorithms for the Digital Controller. These new numbers makes it easy to take advantage of symmetry in the link configuration about the X axis. This reduces the number of equations to be solved and thereby reduces computational time and program requirements. Although this symmetry may not exist for offset conditions, since the precision transformation is always made from a zero base in which symmetry does exist, the computational savings is possible. If the link configuration is changed so the symmetry no longer occurs, the algorithms in the All Digital Controller must be charged and the computational load will increase, although not to the extent that the change could not be accomodated.

It may be confusing to those less familar with the program that the change in link length is expressed in degrees. This angular rotation is ofthe motor, tachometer and encoder used in the actuator. The conversion factor is that 360 degrees of rotation equals .2 inch change in length of the actuator. Thus the length of the actuator

corresponding to .1 deg. is 55.5 micro-inches or 1.41 micro-meters. To achieve 0.1 arcsecond accuracy at the mirror requires controlling each actuator length to 0.22 micro-meters rms or better.

3.1.2 ACTUATOR CONTROL LOOP ANALYSIS

A discussion of the actuator control loop design is contained in Section 2.1.4. Figure 3.1-2, which shows the SOT actuator dynamic model, including structural mode, and Figure 3.1-3, which defines the control approach and the states utilized in the computer, are duplicated in that section. This section provides responses which were obtained on a computer simulation study, using the control loop configuration of Figure 3.1-3 and the dynamic system model of Figure 3.1-2. Parameters used for the actuator control runs are presented on Table 3.1-6. Most of the simulation runs were made with an inertia wheel added to the system to increase the inertia by a multiple of 10. The large inertia enabled a re-distribution of gain so that with bandwidth held constant, friction had 1/10 the effect it previously had. This is further discussed in Section 2.1.4.

Figures 3.1-4 through 3.1-6 were all made with the large inertia but with the rate and displacement gains adjusted together to provide nearly constant displacement bandwidth while the bandwidth of the rate loop varied over a 4 to 1 range. There is no great difference between

X_1 = actuator position
X_2 = actuator rate
X_3 = differential angle representing structural mode
$X_4 = \dot{X}_3$
X_5 = torque motor output (ft. lbs.)

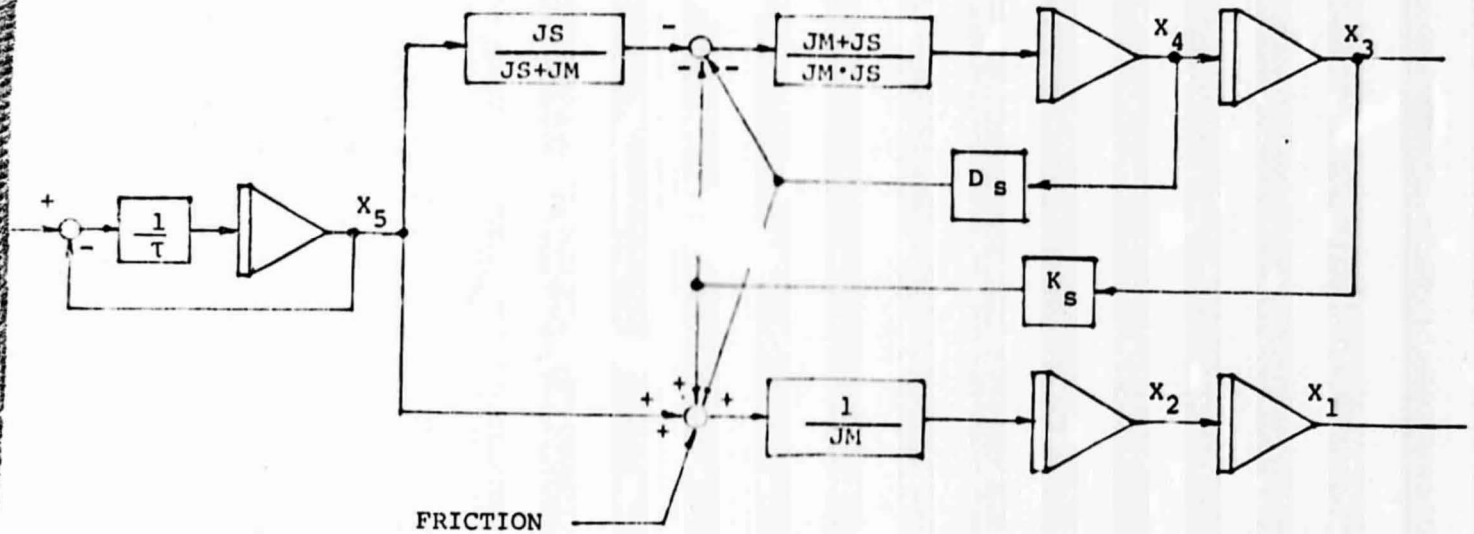

FIGURE 3.1-2: SOT Actuator Dynamic Model Including Structural Mode

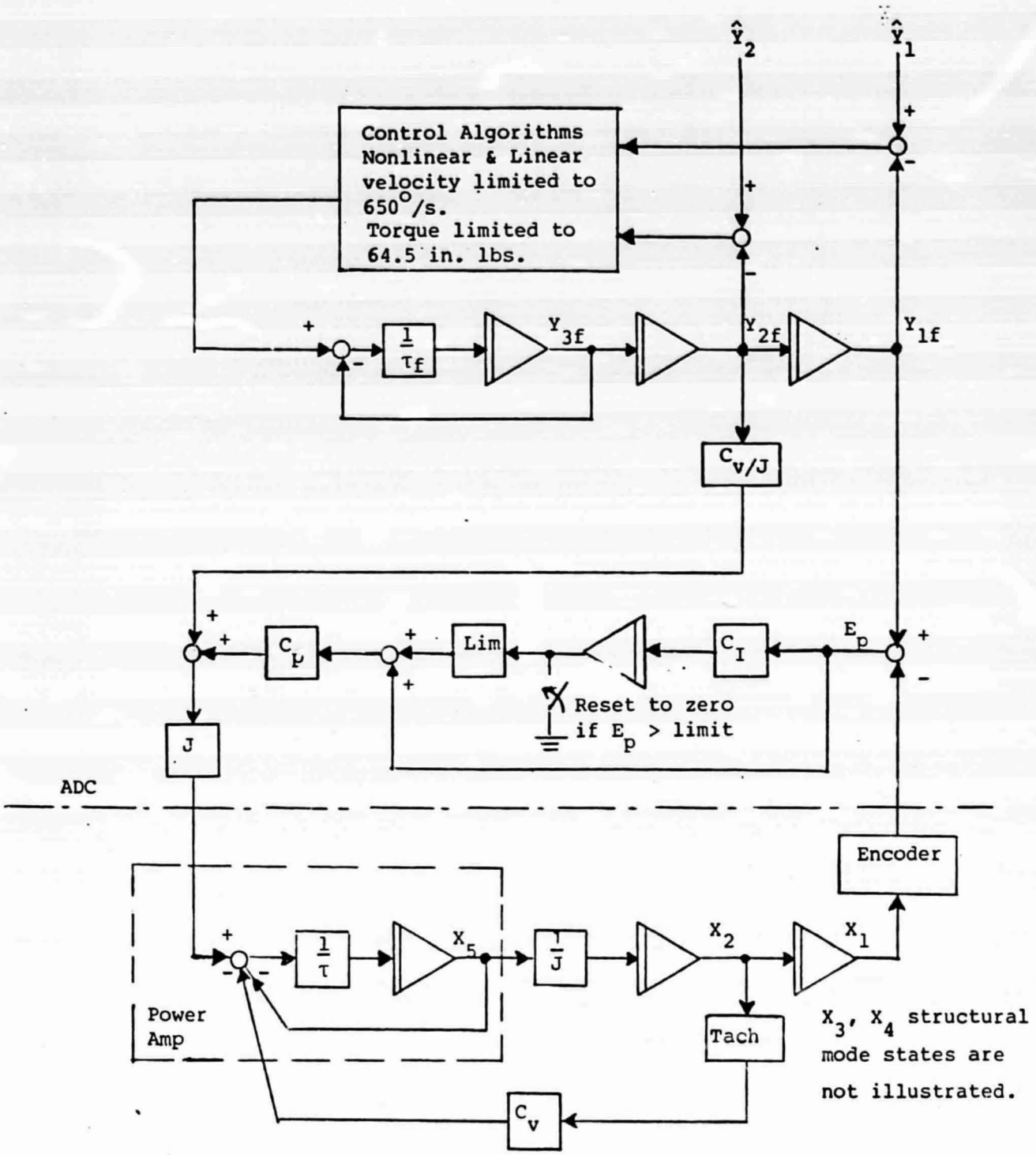

FIGURE 3.1-3: Actuator Loop Control Approach Using Tach Feedback

TABLE 3.1-6: Parameters for Actuator Control Runs
(Except as Noted on Run)

A. Model Parameters

1) Torque Filter = 6 m seconds

2) Nominal B.W. = 15 Hz

3) Velocity Limit = $650^{o}/s$

4) Torque Limit = 64.5 in. lbs.

5) Inertia = Jm + Jw = .137 in. oz. sec^2

6) Low Inertia = Jm = .0137 in. oz. sec^2

B. States of Interest Other Than System States

Y1H = commanded angle = $\hat{Y}_1$

Y2H = commanded angular rate = $\hat{Y}_2$

X6T = Friction estimate

Ep = Error between actual angle and estimate

UT = Torque command

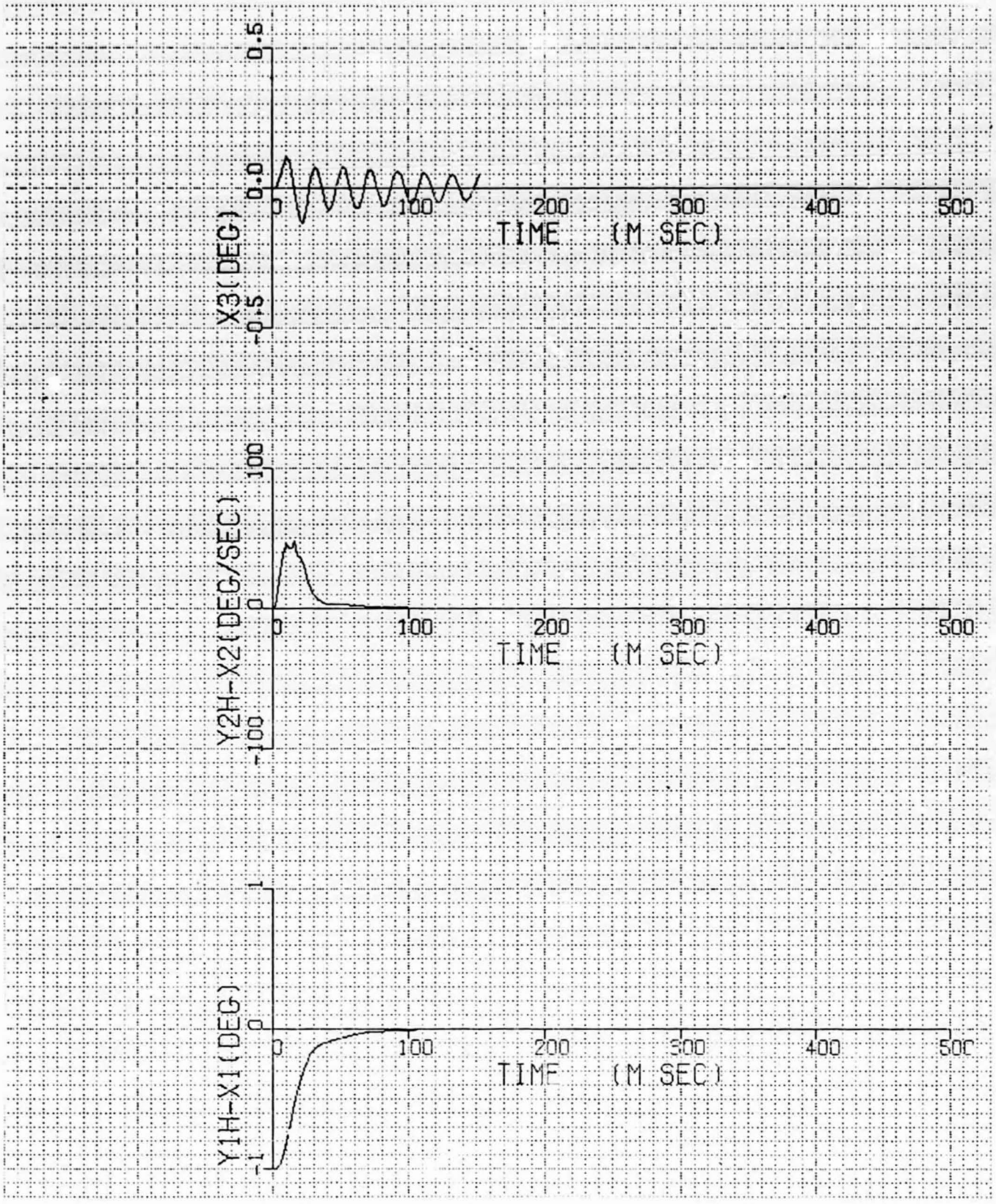

FIGURE 3.1-4A

12.6 HZ LOOP WITH TACH FEEDBACK
(VELOCITY LOOPS B.W. IS 1600 HZ)

RESPONSE TO 1° COMMANDED STEP OF POSITION ERROR, VELOCITY ERROR AND STRUCTURAL MODE.

12/20/79

10:56:14

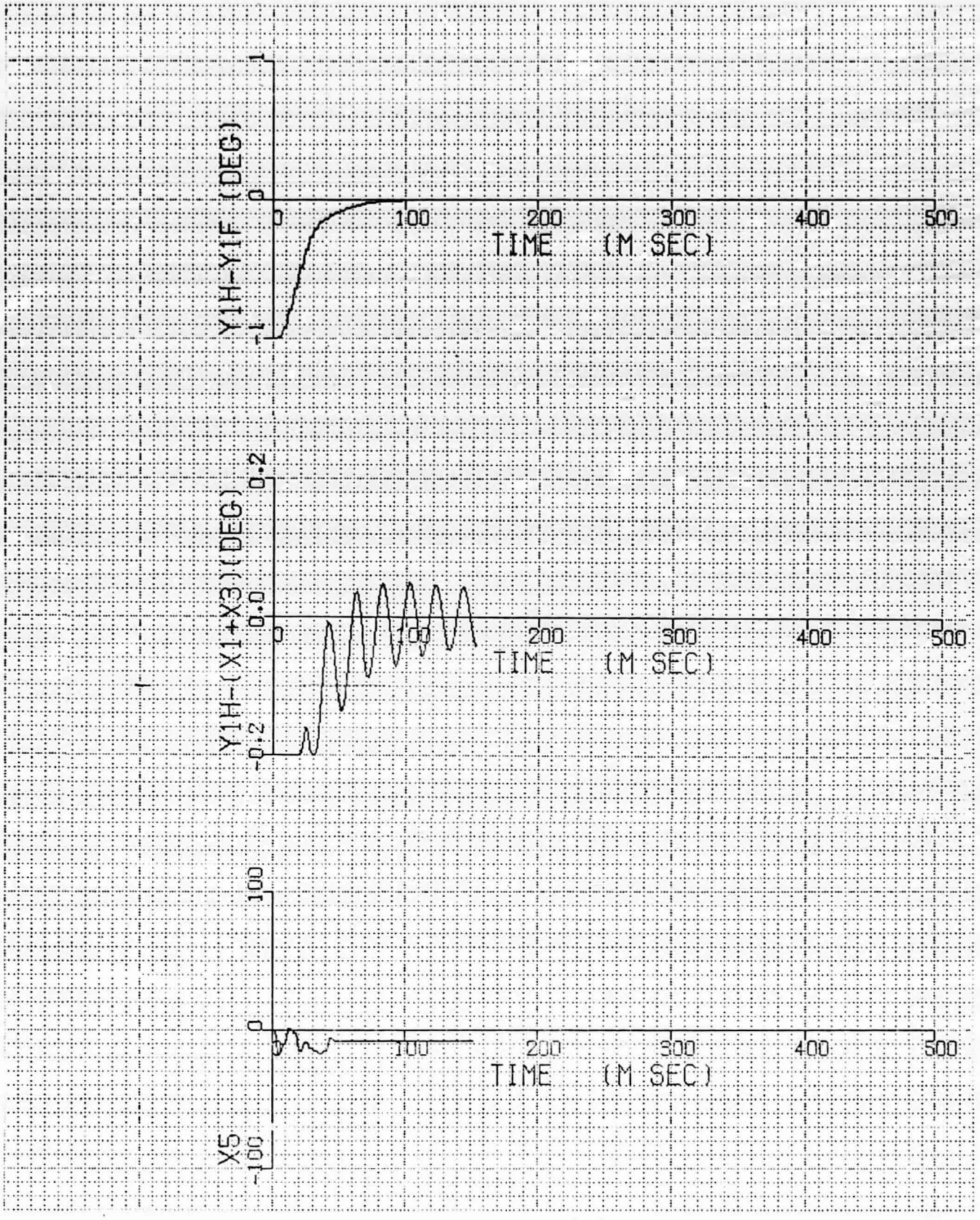

FIGURE 3.1-4B

12.6 HZ LOOP WITH TACH FEEDBACK(VELOCITY LOOP B.W. IS 1600 HZ)

RESPONSE TO 1° COMMANDED STEP OF TORQUE, MIRROR POSITION ERROR AND VELOCITY OF FILTER.

12/20/79 10:56:14

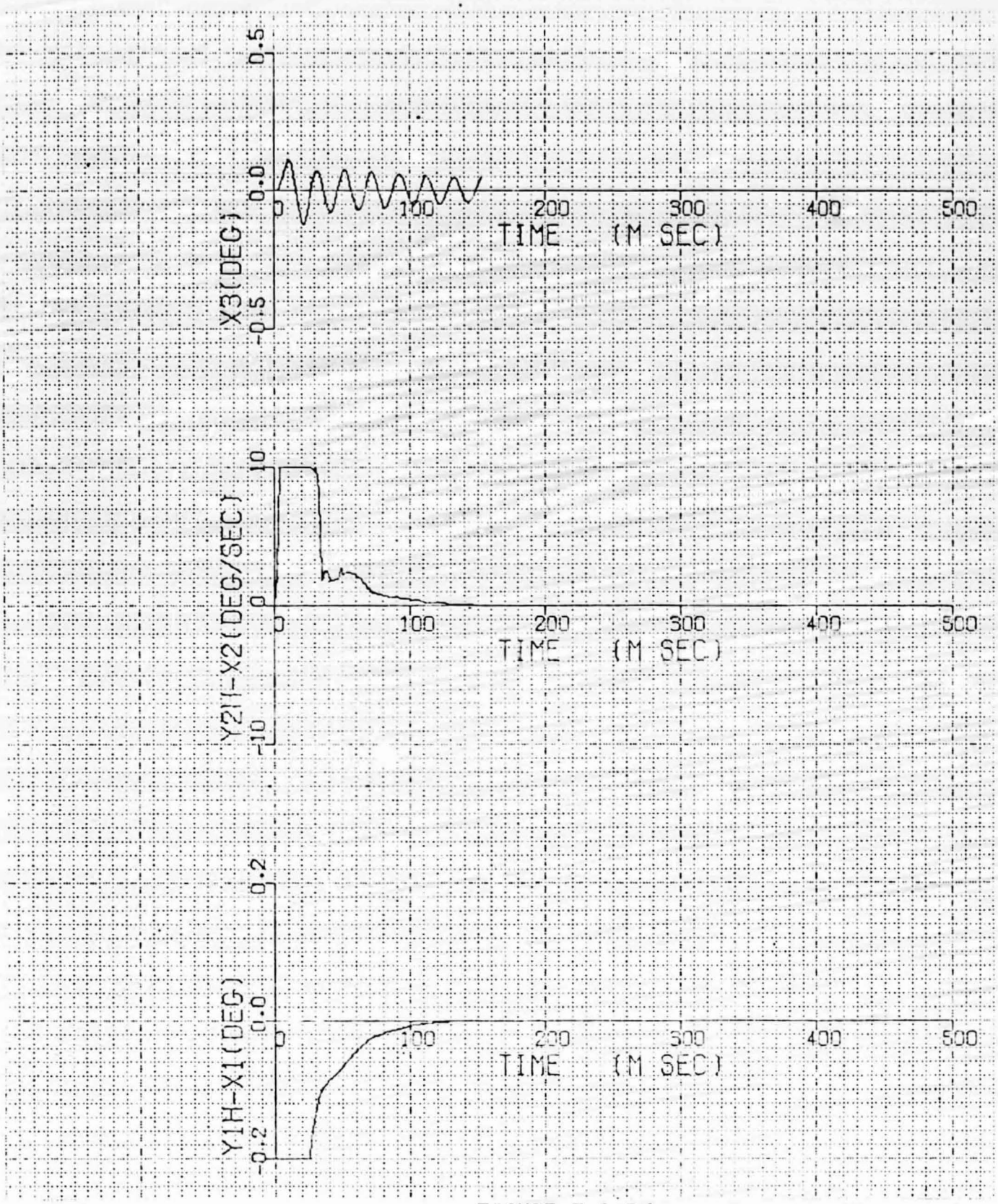

FIGURE 3.1-5 A

12.7 HZ LOOP WITH TACH FEEDBACK (VELOCITY LOOP B.W. IS 800 HZ.)

RESPONSE TO 1° COMMANDED STEP OF POSITION ERROR, VELOCITY ERROR ON STRUCTURAL MODE.

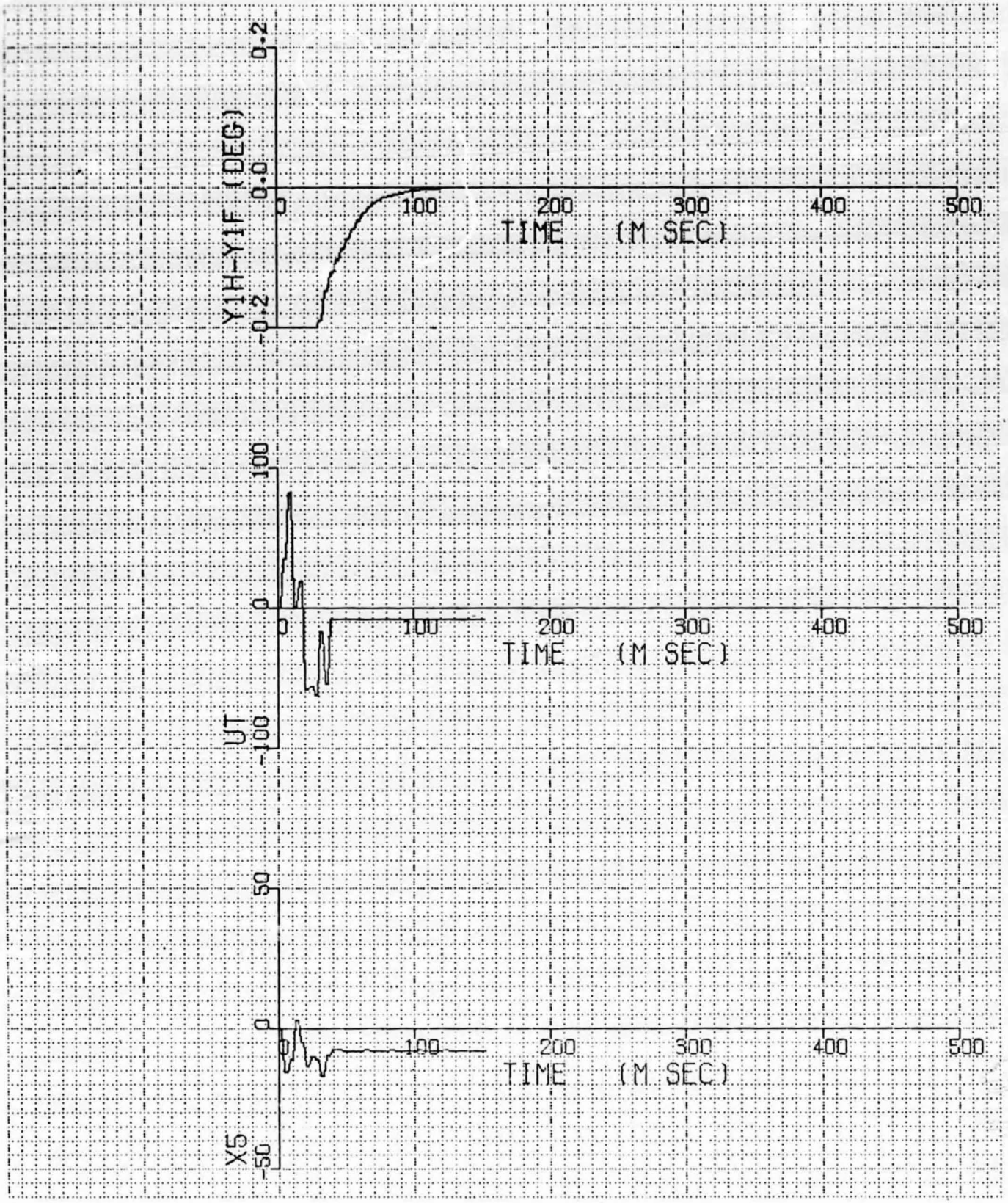

FIGURE 3.1-5B

12.7 HZ LOOP WITH TACH FEEDBACK (VELOCITY LOOP B.W. IS 800 HZ)

RESPONSE TO 1° COMMANDED STEP OF TORQUE, VELOCITY COMMAND AND VELOCITY OF FILTER.

12/14/79 9:49:57

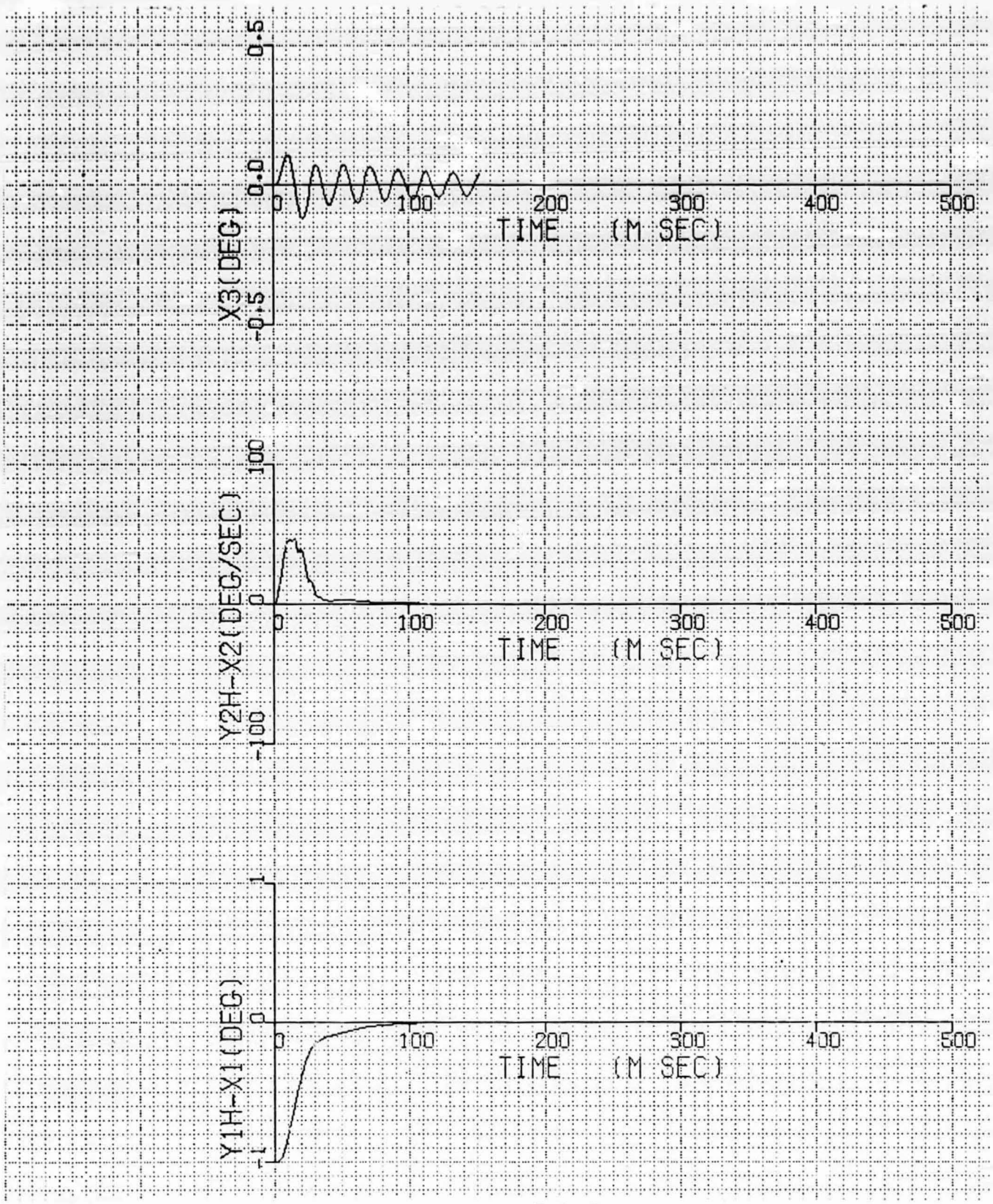

FIGURE 3.1-6

12.9 HZ LOOP WITH TACH FEEDBACK (VELOCITY LOOP B.W. IS 400 HZ.)

RESPONSE TO 1° COMMANDED STEP OF POSITION ERROR, VELOCITY ERROR AND STRUCTURAL MODE.

1/19/80

the responses for these three runs. Referring to the trace for state X_3, note that for a 1^o step the excitation of the structural mode, although noticeable, is within acceptable bounds, (A 1^o step at the actuator is less than 1 arc second step on the mirror.) The activity seen is well below 0.1 arc second, If a 1 arc second step was commanded at the mirror, then several actuators would step togehter. No data is presently available on the amplitude of mirror oscillation for this type input.

For the run of Figure 3.1-7 the inertia wheel was omitted and the gain adjusted to obtain the indicated bandwidth. The result is a stand-off in position error, Y1H - X1, of approximately .15 degeees. The integation gain should eventually drive this error to zero but it would have taken some time. Figure 3.1-8 shows that if the velocity loop bandwidth is increased low inertia does not adversely affect system results.

If wide velocity loop bandwidth can be tolerated, there is no need to add an inertia wheel. The amount of bandwidth that can be tolerated is dependent on noise in the system, mechanical structure rigidity between motor and tachometer, and the time constant of the motor. Although a current drive will reduce the motor time constant it does not bring it to zero since infinite voltage is not available. This is especially true for a

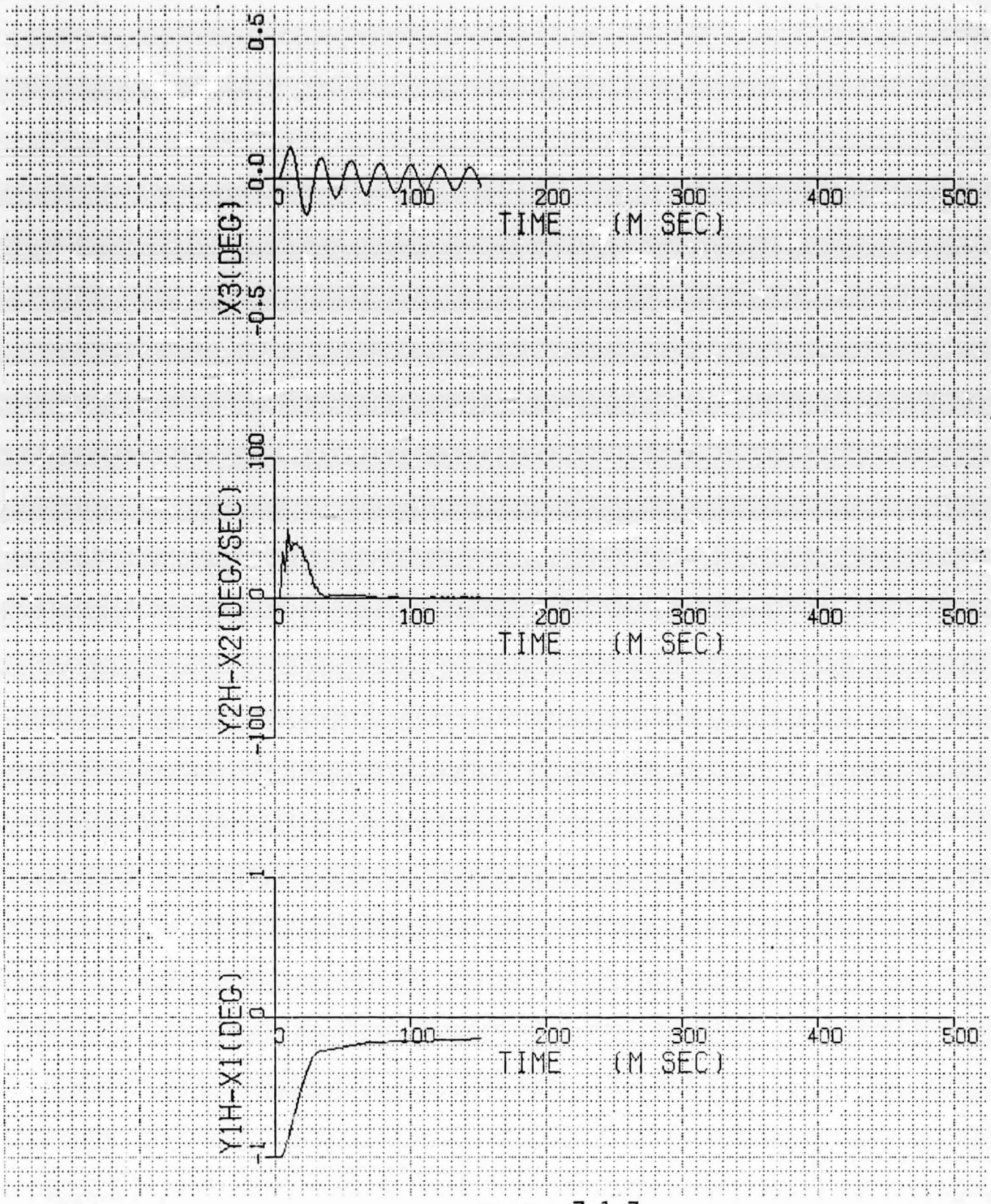

FIGURE 3.1-7
12.9 HZ LOOP WITH TACH FEEDBACK BUT LOW INERTIA
(VELOCITY LOOP B.W. IS 400 HZ)

RESPONSE TO 1° COMMANDED STEP OF POSITION ERROR, VELOCITY ERROR AND STRUCTURAL MODE.

1/19/80

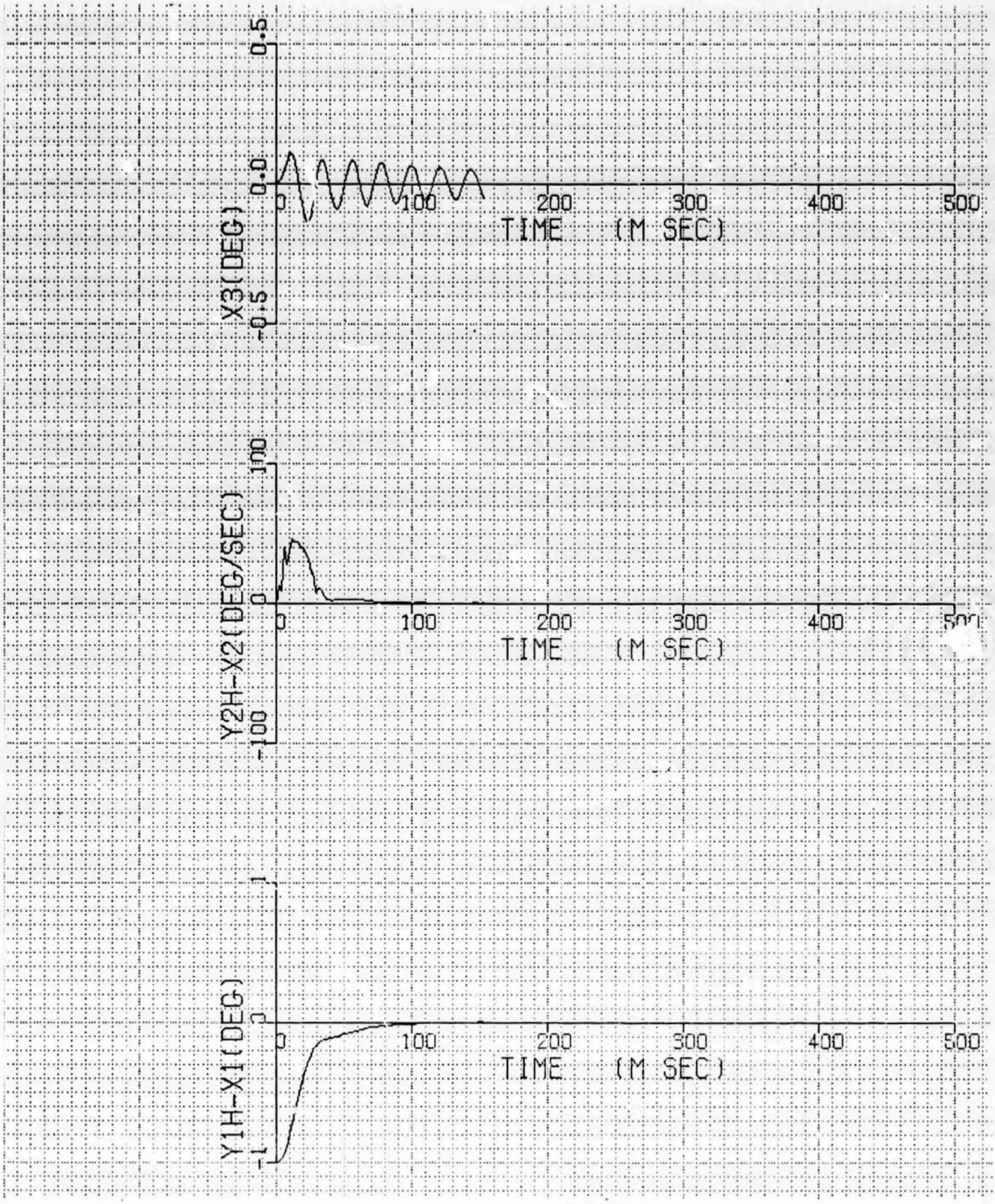

FIGURE 3.1-8

12.6 HZ LOOP WITH TACH FEEDBACK BUT WITH LOW INERTIA.
(VELOCITY LOOP B.W. IS 1600 HZ)

RESPONSE TO 1° COMMANDED STEP OF POSITION ERROR, VELOCITY ERROR AND STRUCTURAL MODE.

1/19/80

00:08:26

pulse width amplifier of the type planned for SOT. All the runs presented here included in the simulation a rough approximation of the characteristics of the power amplifier. Thus, it is expected that these responses will hold reasonably well in the actual system.

The response of the system to a 1^{o} offset of position error is illustrated on Figure 3.1-9. This is similar to the step response except that a step command is filtered by the follow up model which is not true of the offset response. Therefore, there is much greater excitation of the structural mode. This is clearly evident in the X_3 trace, which represents the difference angle between opposite ends of the "structural spring."

The response of the system to a large step, 100^{o}, is illustrated on Figure 3.1-10. The system has a soft limit in velocity of 650^{o} per second. The velocity is limited only by placing a limit on the position error in the follow up model. However, the system lags slightly behind the follow up model initially, builds up a position error, and this causes the velocity to overshoot. A slight complication of the algorithms could eliminate this. However,in the SOT system it is not felt that this creates a problem. Note that for the large step the structural mode excitation is increased. This is due to the larger torque input. A larger step does not result in a porportional increase in torque and so would

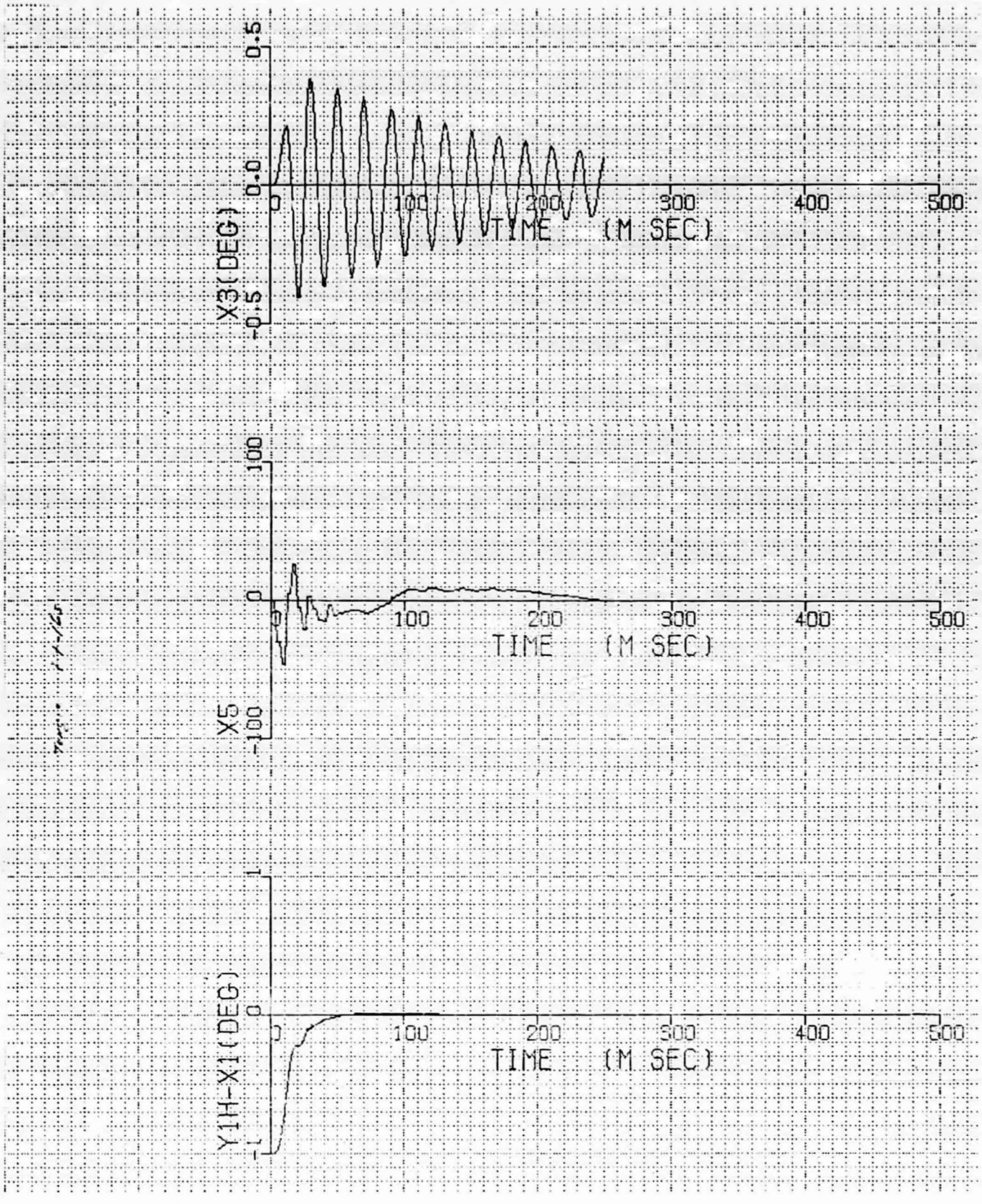

FIGURE 3.1-9 12.6 HZ LOOP WITH TACH FEEDBACK (VELOCITY LOOP B.W. IS 1600 HZ)

RESPONSE TO 1° OFFSET OF POSITION ERROR, TORQUE AND STRUCTURAL MODE.

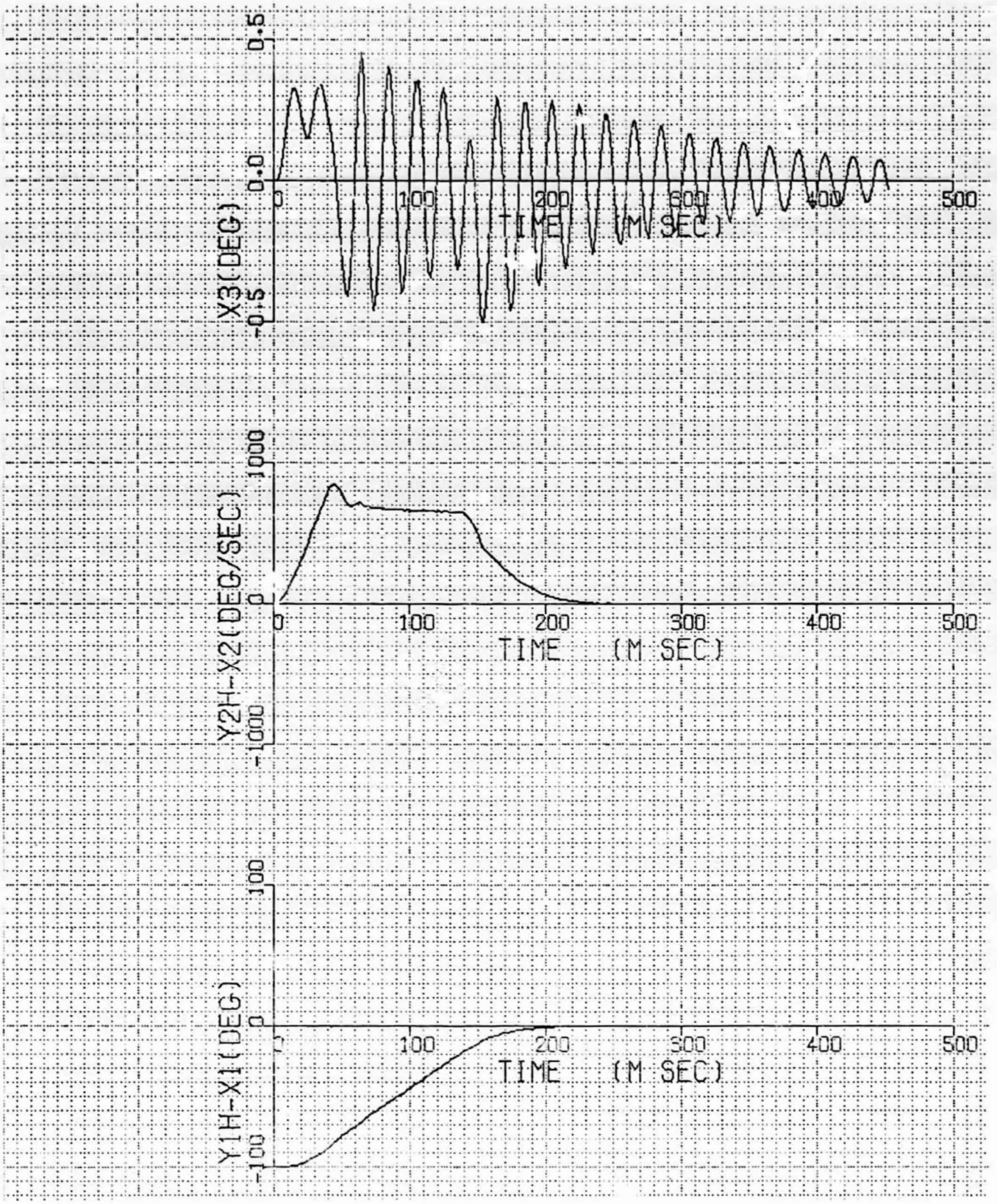

FIGURE 3.1-10: 6.3 HZ LOOP WITH TACH FEEDBACK (VELOCITY LOOP B.W. IS 1600 HZ)
RESPONSE TO 100° COMMANDED STEP OF POSITION ERROR, VELOCITY ERROR AND STRUCTURAL MODE.

12/17/79 18:07:39

not result in a proportionally larger amount of excitation.

The actuator assembly received from the Sacramento Peak Observatory had a X19 inertia wheel installed. To see what effect this would have on loop response, the run of Figure 3.1-11 was made. No great difference between this and the runs of Figure 3.1-4, 5 and 6 can be noted.

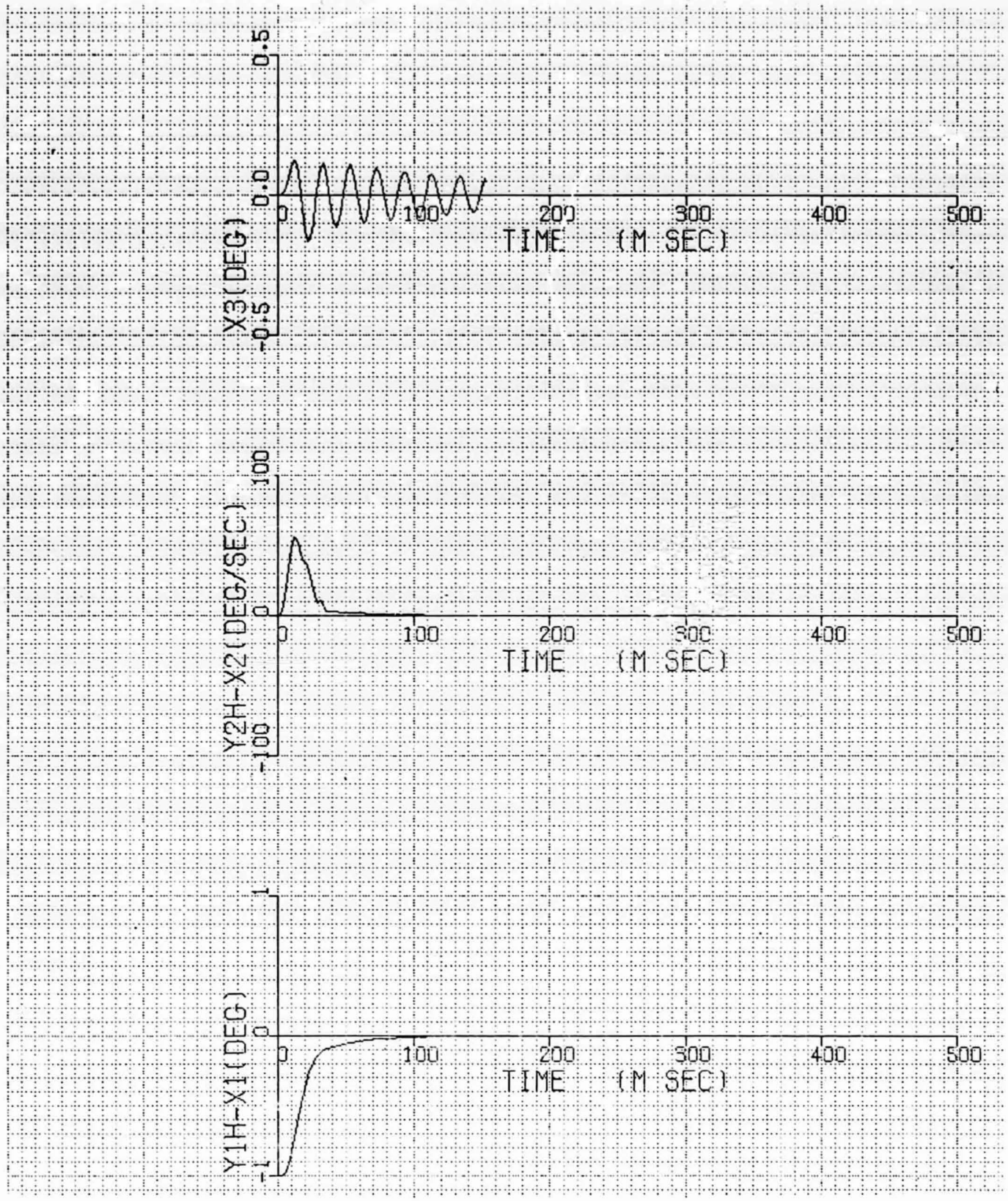

FIGURE 3.1-11

12.9 Hz LOOP WITH TACH FEEDBACK
(VELOCITY LOOPS B.W. IS 400 Hz)

RESPONSE TO 1° COMMAND STEP OF POSITION ERROR, VELOCITY ERROR AND STRUCTURAL MODE. (19 X INERTIA)

3.2 COMPUTER PROGRAM DEFINTION

3.2.1 MEMORY ALLOTMENT

Table 3.2-1 defines the present allocation for the instructions in program memory. In spite of the high complexity of the transformations involved and control algorithms for 6 loops, only 1022 words of instructions are required. Note that any increase in memory, such as for initialization or any housekeeping routines, result in exceeding the original 1024 words in the Digital Controller memory. It was for this reason that program memory capacity was increased to 4K for the SOT application. Bearing in mind the complexity of the program contained in 1K of program memory, it is difficult to imagine exceeding the 4K capacity now in the Digital Controller planned for SOT. However, the memory is readily expandable in 4K pages up to 65K, should further expansion be required.

The allocation of words in data memory is illustrated on Figure 3.2-1. As indicated, the memory can be segmented into 8 sets. Six of these 8 sets are assigned to the 6 actuator control loops, 6 sets of transformation equations, one for each link, and equations for estimating the 5 sensors, and are all indexed "loop"parameters. For these 6 loops there are 128 word locations per set, leaving 29 locations per set not used. Two of the 8 sets are non indexed and they include 64 constants and 32 variables. Here, an

TABLE 3.2-1: Program Memory Allocation

Routine	No. of Instructions
A. Control Algorithms (6 loops)	346
B. Transformations	
1) Sensor Meas. and K-Filter	73
2) "Precision" Transformation	431
3) "Fast" Transformation	45
Sub-Total	549
C. Desired Link Length Calculation	16
D. Update Fast Transformation	60
E. Miscellaneous such as general sub-routines, jump tables, etc.	51
Total	1022

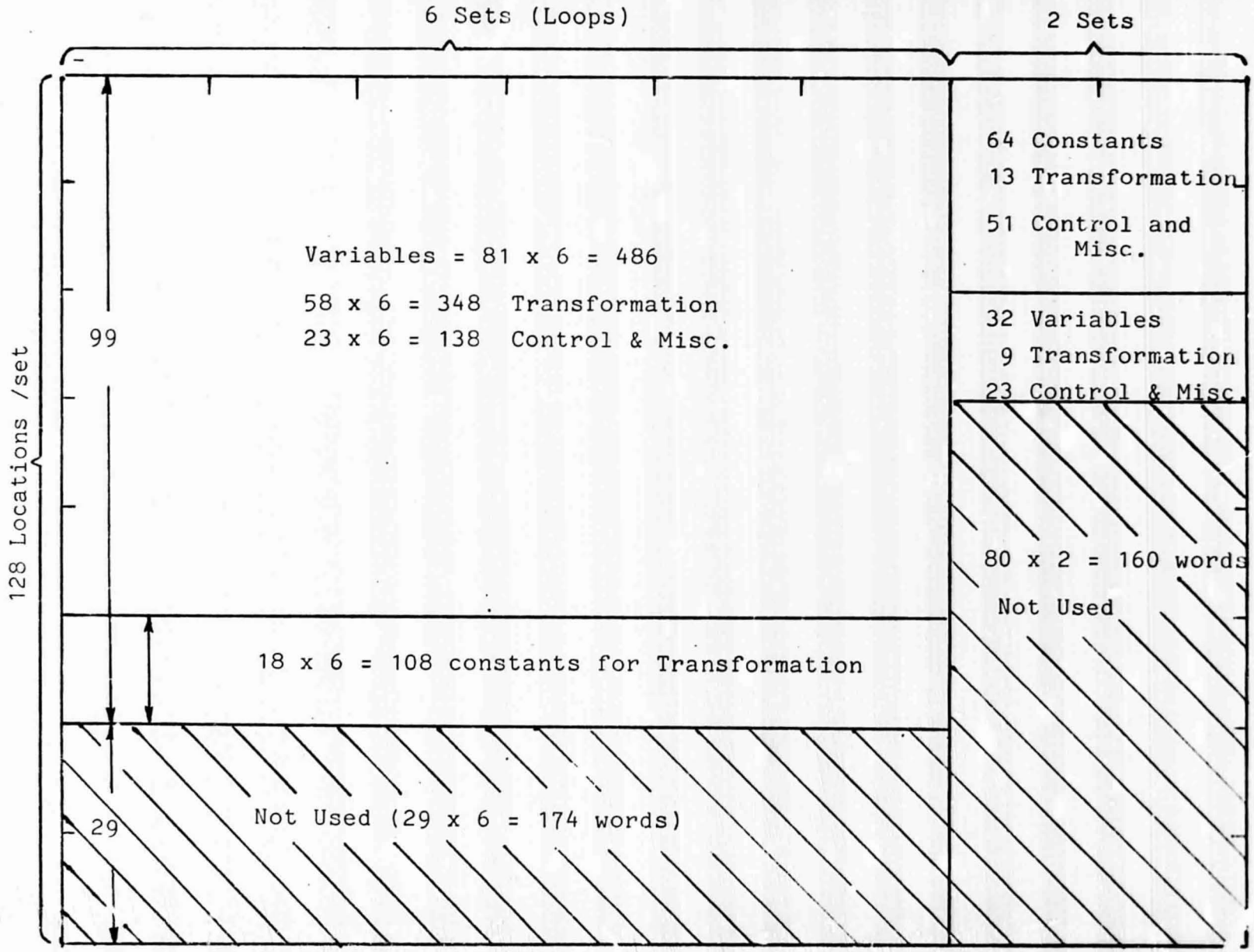

FIGURE 3.2-1: Data Memory Allocation

additional 160 words of data memory are not used making a total of 334 words unused in the first 1K of data memory. Since in the SOT system 2K of data memory is provided, over half of data memory remains available for use. Data memory can readily be expanded to 4K and even further using paging techniques.

3.2.2 TIMING RESULTS

The instructions involved in various routines in the program for the Solar Optical Telescope were divided into sets of Multiply, Divide, Shift, IO and "Other Instructions," and the number in each set counted. The number of instructions in each set was multiplied by the time required to execute that instruction to provide the total time required to execute that program routine. This was compared with time measured using a logic analyzer. The results of this are given on Table 3.2-3.

In most of the sets of instructions there are variations in path lengths. It was planned that the calculation time should include the maximum path length. No effort was made on the measured time to assure it was maximum. Thus the calculated time should always exceed measured time but in one particular case this was not true. It is apparent that a small error was made either in measuring or calculating the time required to perform the link length extrapolation algorithms.

Figure 3.2-2 illustrates the program sequence for

ROUTINE	Multiple Cycle Instruction			Single Cycle Instruction		Execution Time (micro sec)	
	MULT	DIV	Shift	I/O	Other	CAL	Meas.
A. Control Algorithms	126	0	180	1995	14	1147	1102
B. Transformations	320	6	345	4187	10	2464	2395
C. Link length Extrapolation	6	0	6	90	0	54	60
D. "Fast Trans" update	42	6	36	280	0	287	283
Path A + B	446	6	525	6182	24	3611	3497
Path A + C	132	0	186	2085	14	1201	1162
Path A + C + D	174	6	222	2365	14	1488	1445

TABLE 3.2-2 : SOT Computational Time Requirement

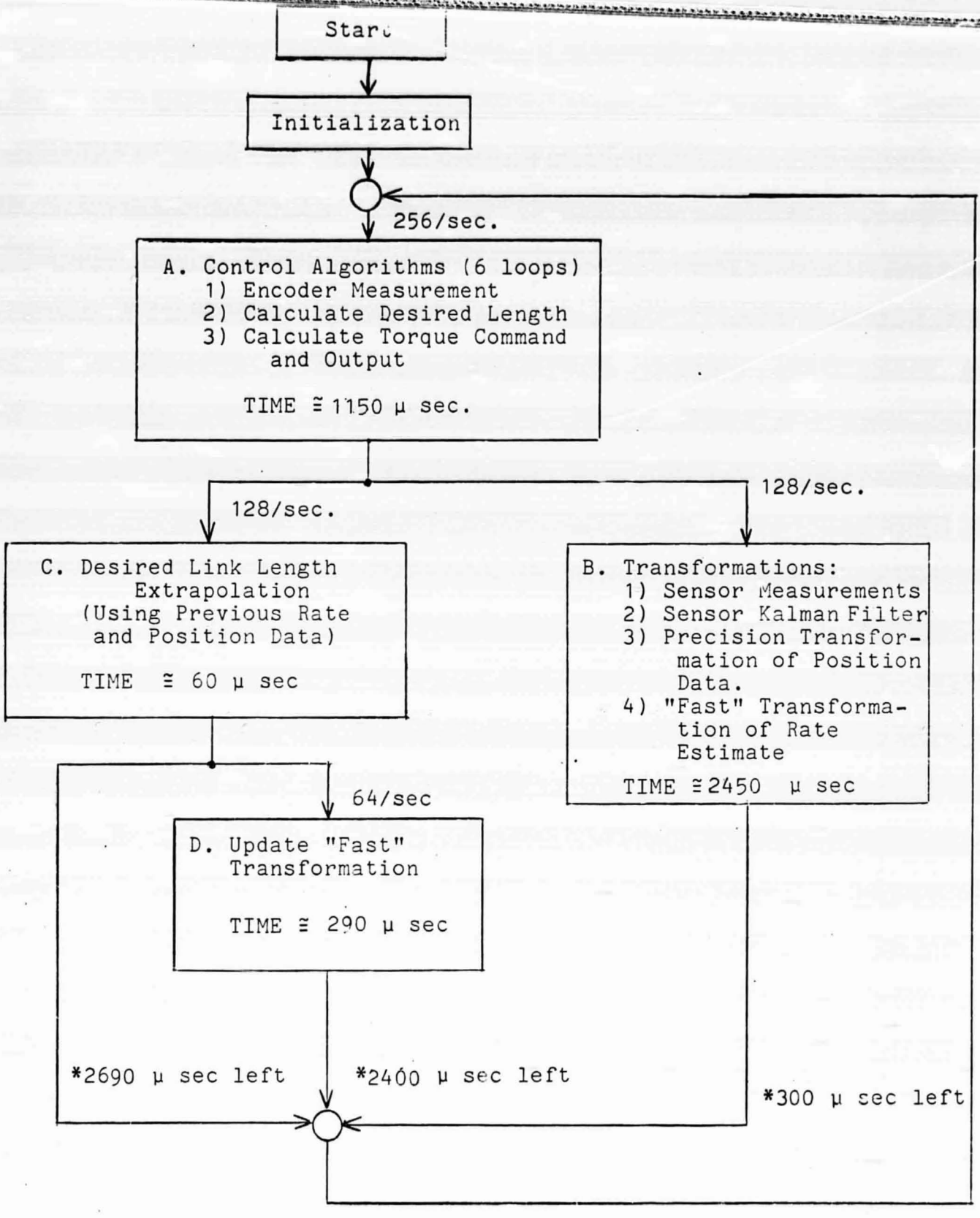

FIGURE 3.2-2:SOT Control Program Sequence

* Time remaining during one 3900 μ second cycle for other tasks.

SOT program. Each of the computational sets included in the blocks correspond to the sets listed on Table 3.2-3. The times provided on Figure 3.2-2 are rounded off somewhat from the figures on the table, but are meant to be conservative. The conclusion to be drawn from Figure 3.2-2 is that there is considerable amount of computation time left which can be allocated to performing other SOT tasks. If additional time was required the precision transformation could be performed at a lower rate utilizing the fast transformation for small changes in the interim period between precision transformation updates. Navtrol believes that with the time available now, plus additional time obtained, if necessary, by reducing the rate of computation for the precision transformation, that foreseeable control tasks, such as pointing the LOS guider and etc. could be accomplished within a single Digital Controller.

3.3 HARDWARE RESULTS

3.3.1 COMPUTER RESULTS

Results provided in Section 3.1.1 and Section 3.2 demonstrated that the Digital Controller Processor unit was capable of performing the required calculations with sufficient speed and accuracy so that the known SOT requirements can all be met using a single Digital Controller. With the increase in memory size of the processor unit, sufficient spare memory capacity exists to handle all foreseeable requirements. Though these results are reported in other sections they are truly hardware results since they define the computer capabilities required to perform the SOT functions.

Table 3.3-1 summarizes the specific characteristics of the SOT Processor Unit. Detailed characteristics of the Digital Controller in general are in Appendix A.

3.3.2 ACTUATOR CONTROL RESULTS

Section 3.1.2 provided results obtained on simulation studies performed on the CDC Cyber 72 computer. Those results were used to define the algorithms to be programmed into the Digital Controller but also provided a basis of comparison of results obtained on the Digital Controller.

The responses obtained in Figures 3.3-1 through 3.3-8 were made by simulating system dynamics within the All

TABLE 3.3-1

SOT COMPUTER DEFINITION

1. Memory Capacity

   Program Memory; 4K

   Data Memory; 2K

2. Capability

   1. All APM Control Transformations
   2. Control of all 6 Actuator Loops
   3. Measurement of all 5 sensors
   4. Control of LOS Guider or other mechanisms associated with the APM.
   5. Miscellaneous housekeeping and other tasks.

3. Physcial Size

   Three double sided P.C. Boards, 5.6" x 10" mounted in a suitable package estimated to be 2" x 6.5" x 10.5". (A smaller package could be utilized if required.)

4. Processor Unit Power

1.	Arithmetic board	7.4W. @ 5V.
2.	*Memory Board (5K)	15.6W. @ 5V.
3.	Communication I/O	3.7W. @ 5V.
	Total for "Flight" Processor Unit	26.7W. @ 5V.

* Requires 21.0W. with 6K RAM. Total for Development Processor Unit is 32.1W.

Digital Controller. Friction and the structural mode were not included in this simulation, but torque time constant and tachometer feedback were. These results show a close correspondence to results obtained on the CDC Cyber computer. For example, on Figure 3.3-1 the error for 1° position step command is reduced.to $.1^{\circ}$ in 30 to 35 milli-seconds. Comparing this to the analytical results for a similar run, Figure 3.1-4, it is seen that the results match.

Also shown on Figure 3.3-2 is the response of the follow up model position error. The approach taken is to try to force the system to follow this model response. Results show that this was accomplished to a reasonable degree although the position error is less than the follow-up error at 30 milli-seconds. This is because the actual system initially lags behind the model system then overshoots slightly as it recovers. In this case the slight overshoot actually reduced the error at this point.

Figures 3.3-3 and 3.3-4 provide the response of the system to a 100° position step command. This can be compared to Figure 3.1-10. Note that in Figure 3.3-3 approximately 150 milli-seconds is required for the error to be reduced to less then 10 degrees. This corresponds almost exactly to the result obtained in the simulation run.

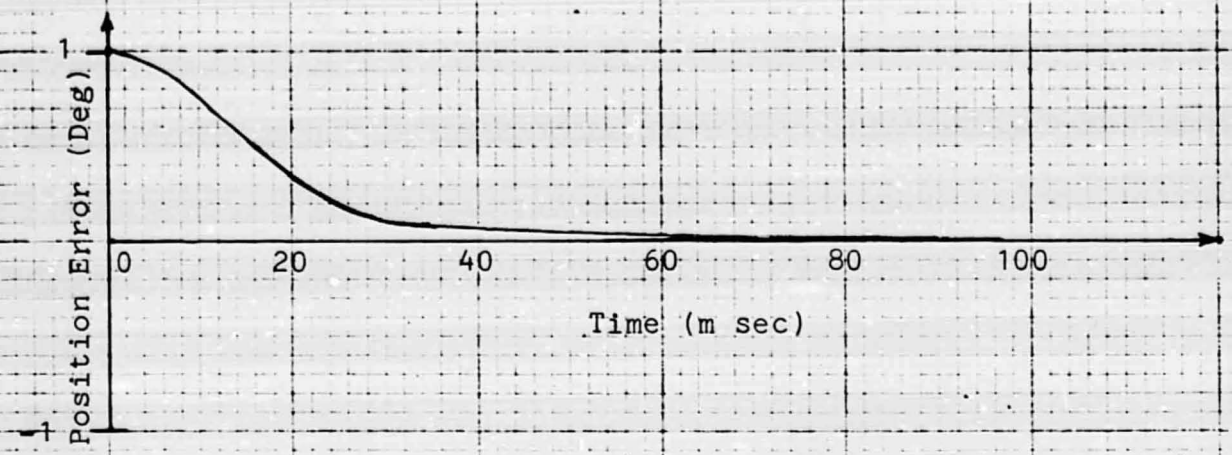

Figure 3.3-1: Position Error of 1^{o} Position Step Command

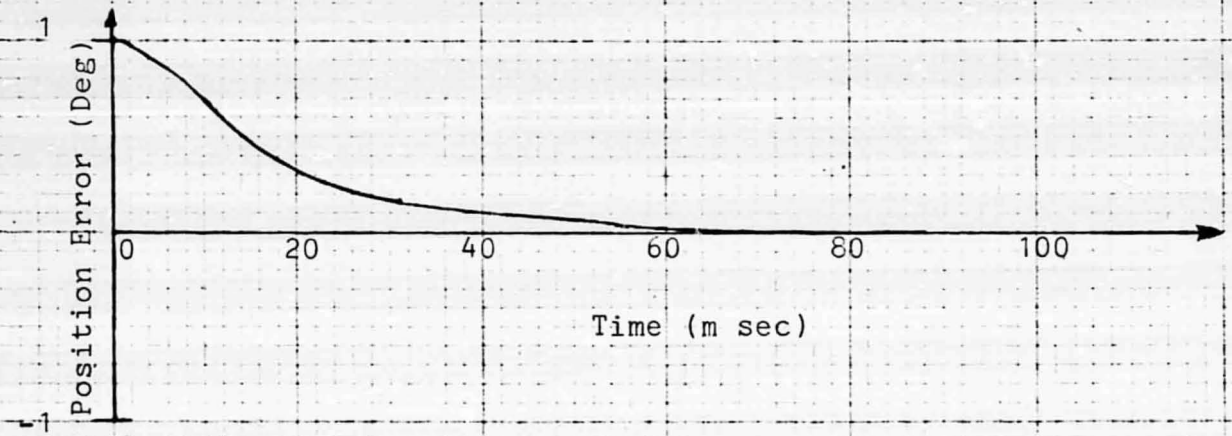

Figure 3.3-2: Follow up Model Position Error of 1^{o} Position Command

C-2

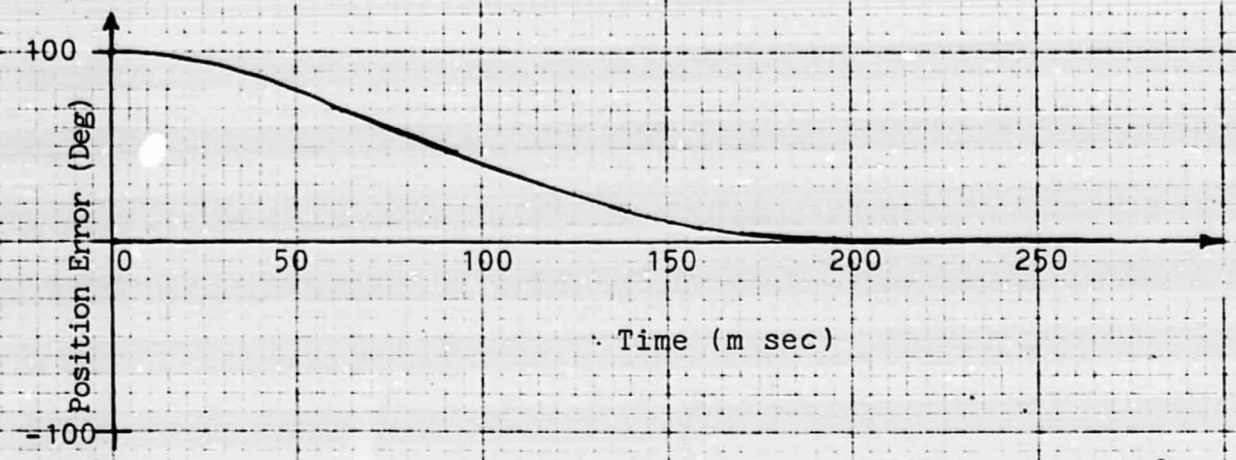

Figure 3.3-3: Position Error of 100° Position Step Command

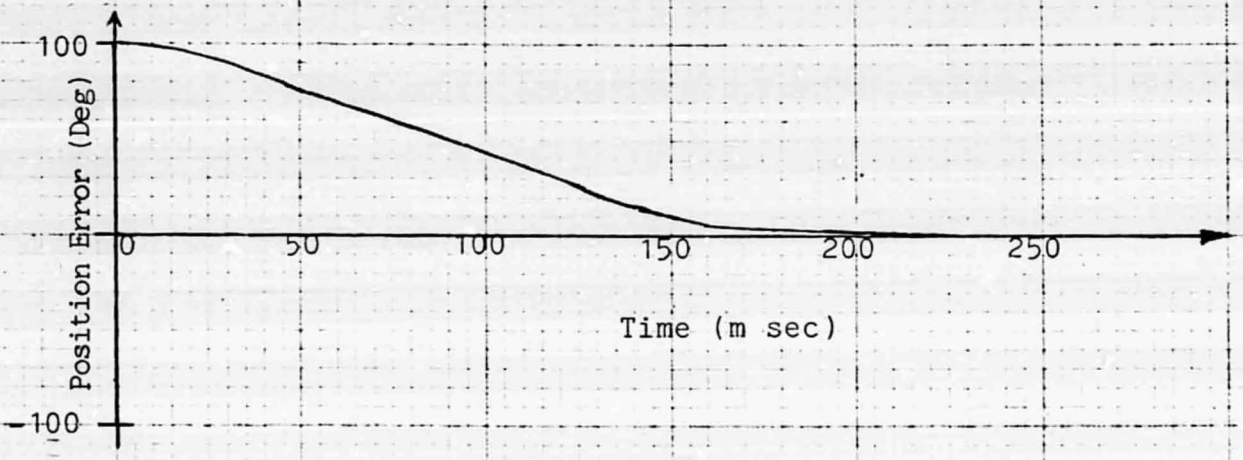

Figure 3.3-4: Follow up Model Position Error of 100° Position Command

Figures 3.3-5 through 3.3-8 demonstrate the system's capability to follow the velocity step command of 100° per second. Loop dynamics and velocity feed forward keep position error build up to less than 1°. Because of the position error the velocity error overshoots in order to bring position error back to zero.

3.3.3 ACTUATOR ASSEMBLY BACKLASH TESTS

These tests were performed by the Sacramento Peak Observatory on the actuator assembly that they constructed. It is reported here only for completeness since it ties in with the control system developed by Navtrol for the APM. The measured friction of the unit shipped to Navtrol was 4.5 in. lb.. Backlash is shown on Figure 3.3-9 and was made using the set up of Figure 3.3-10. Two measurements were made, one with no load and one with a 50 lb. weight.

3.3.4 MOTOR ENCODER INTERFACE RESULTS

The photo cell pre-amplifier board designed by Navtrol was installed in the Baldwin encoder and the unit interconnected to the Motor-Encoder interface module. This, in turn, was tied to the All Digital Controller through the serial communication circuitry. Prior to the overall test, the signals from the encoder preamp were monitored on an oscilloscope to observe the characteristics of the sine and cosine waves. The waves are reasonably sinusoidal and appropriately

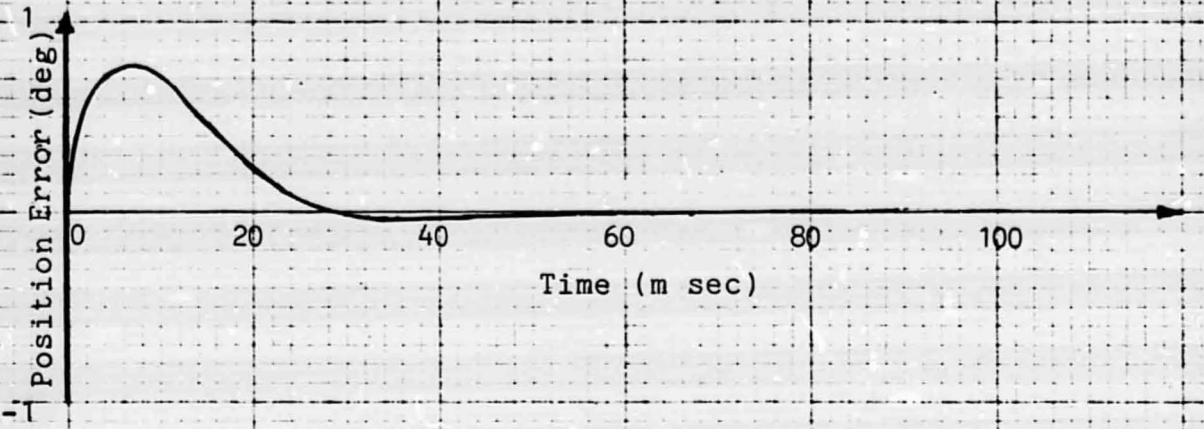

Figure 3.3-5: Position Error of 100°/s Velocity Step Command

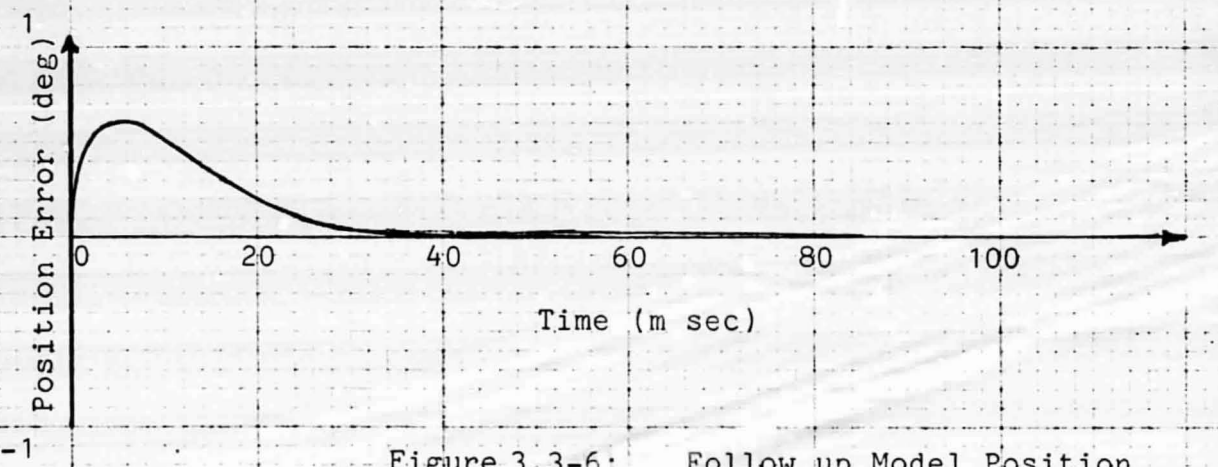

Figure 3.3-6: Follow up Model Position Error of 100°/s Velocity Step Command

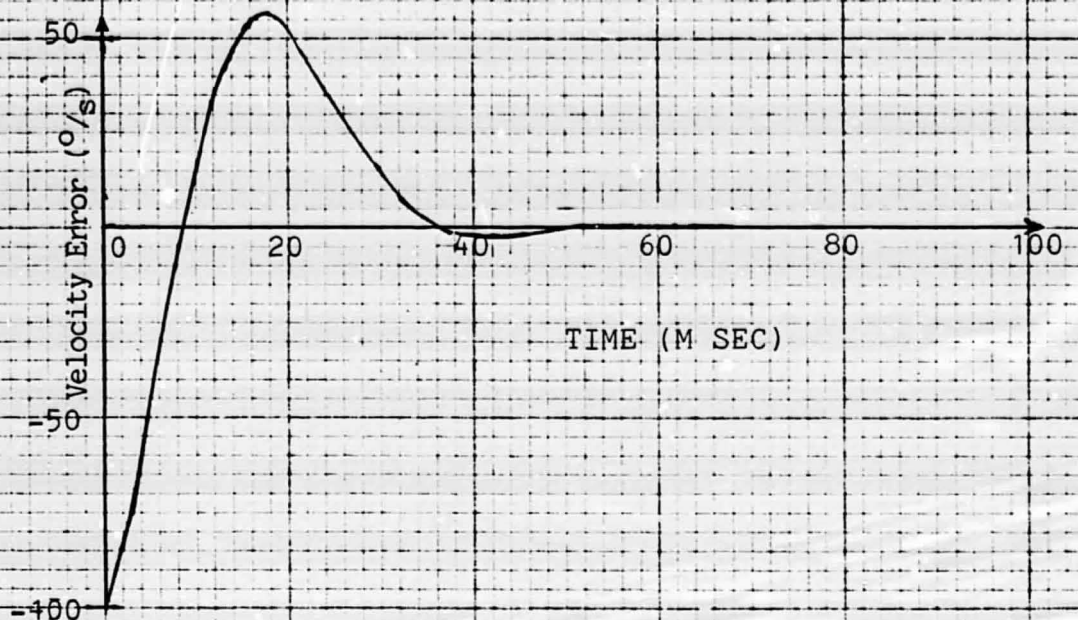

FIGURE 3.3-7: Velocity Error for 100°/s Velocity Step Command

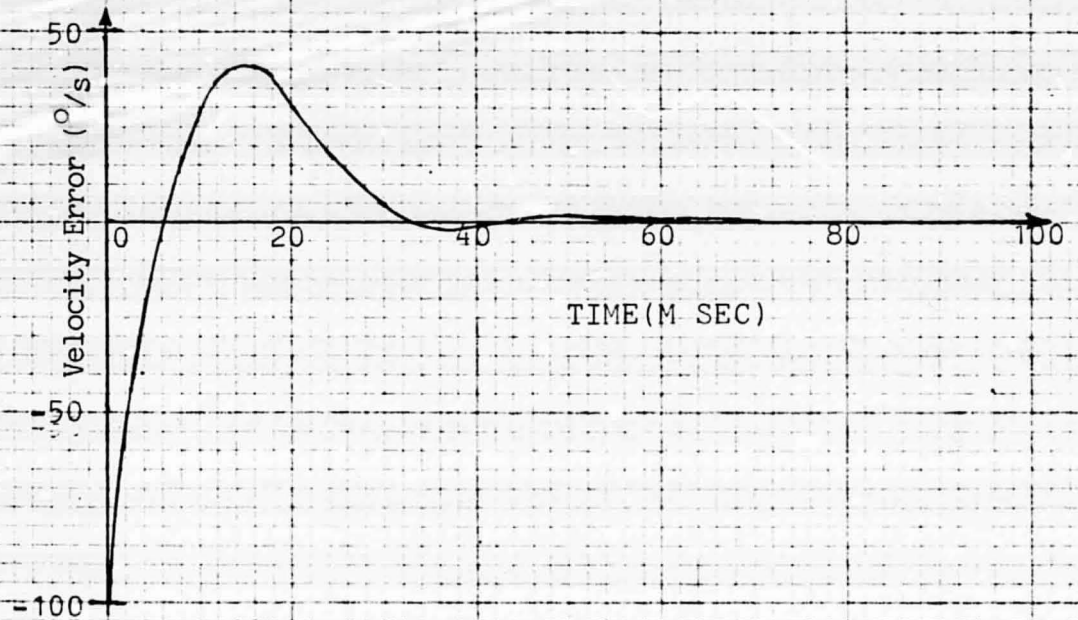

FIGURE 3.3-8: Follow up Velocity Error for 100°/s Velocity Step Command

FIGURE 3.3-9: Backlash Test Result (SPO)

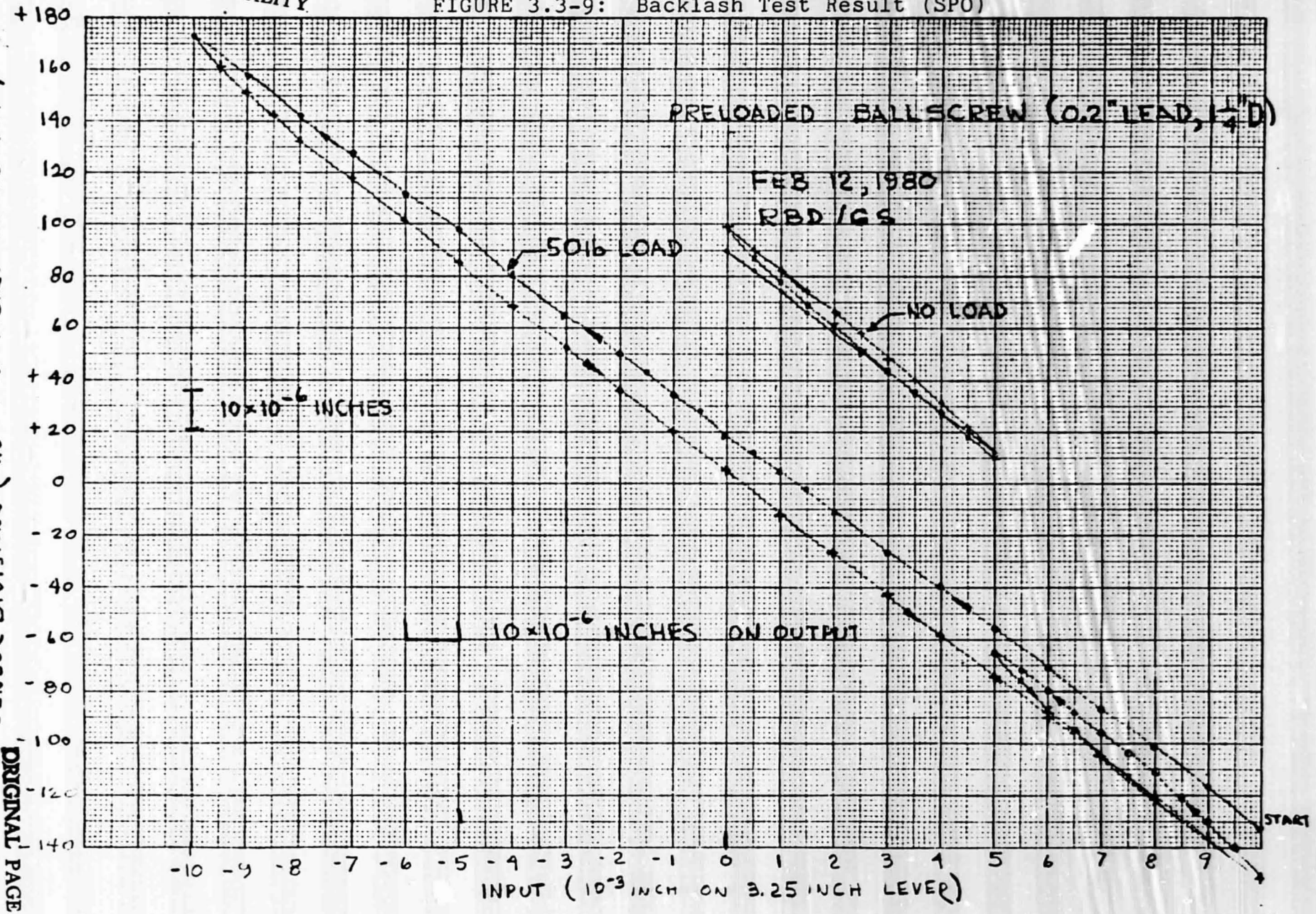

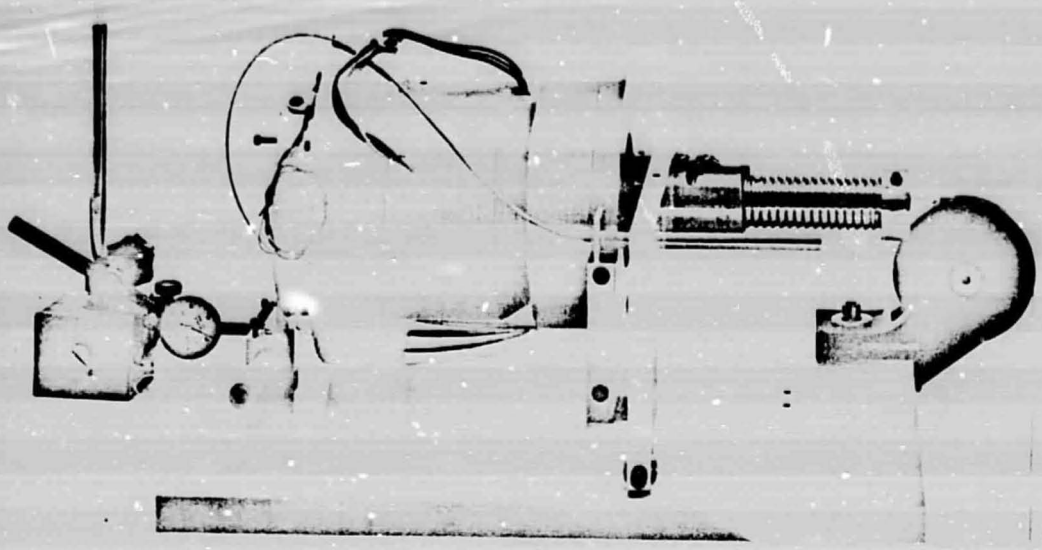

FIGURE 3.3-10
Backlash Test Setup

ORIGINAL PAGE
BLACK AND WHITE PHOTOGRAPH

phased. With the adjustments provided, the amplitude of both the sine and cosine wave could be made equal to each other, and could be made equal about zero. Adjustments for equalizing time above and below zero for the sine and cosine waves were also successful.

After adjustment of the sine and cosine wave the motor commutational phasing was compared to timing of the encoder index pulse. The encoder was rotated slightly to bring the index pulse in coincidence with the zero crossing of the generated voltage from the appropriate winding of the motor so that the commutational signals would be correct. Various angles were then measured using the encoder feeding back to the computer, rotating the motor shaft to vary the angle. This gross accuracy test confirmed the integrity of the overall encoder interface design. The encoder had previously been tested by placing DC signals which corresponded to the sine and cosine of a particular angle into the inputs. These tests verified the capability of the encoder interface to determine accurately the appropriate angles from sine and cosine voltages fed in. It should be noted that in the approach taken the results are approximately independent of the overall amplitudes of the signals. They depend only on relative amplitude of the sine and cosine signals.

The ability of the computer to command torques

has been established. Figure 3.3-11 illustrates the demonstrated linearity of the SOT motor driver power amplifier. Additional test results on the power amplifier are not yet available.

Tests on the actuator and the control of the actuator by the All Digital Controller was not a part of this contract. Although it was hoped that such tests could be included, time and funds did not permit it.

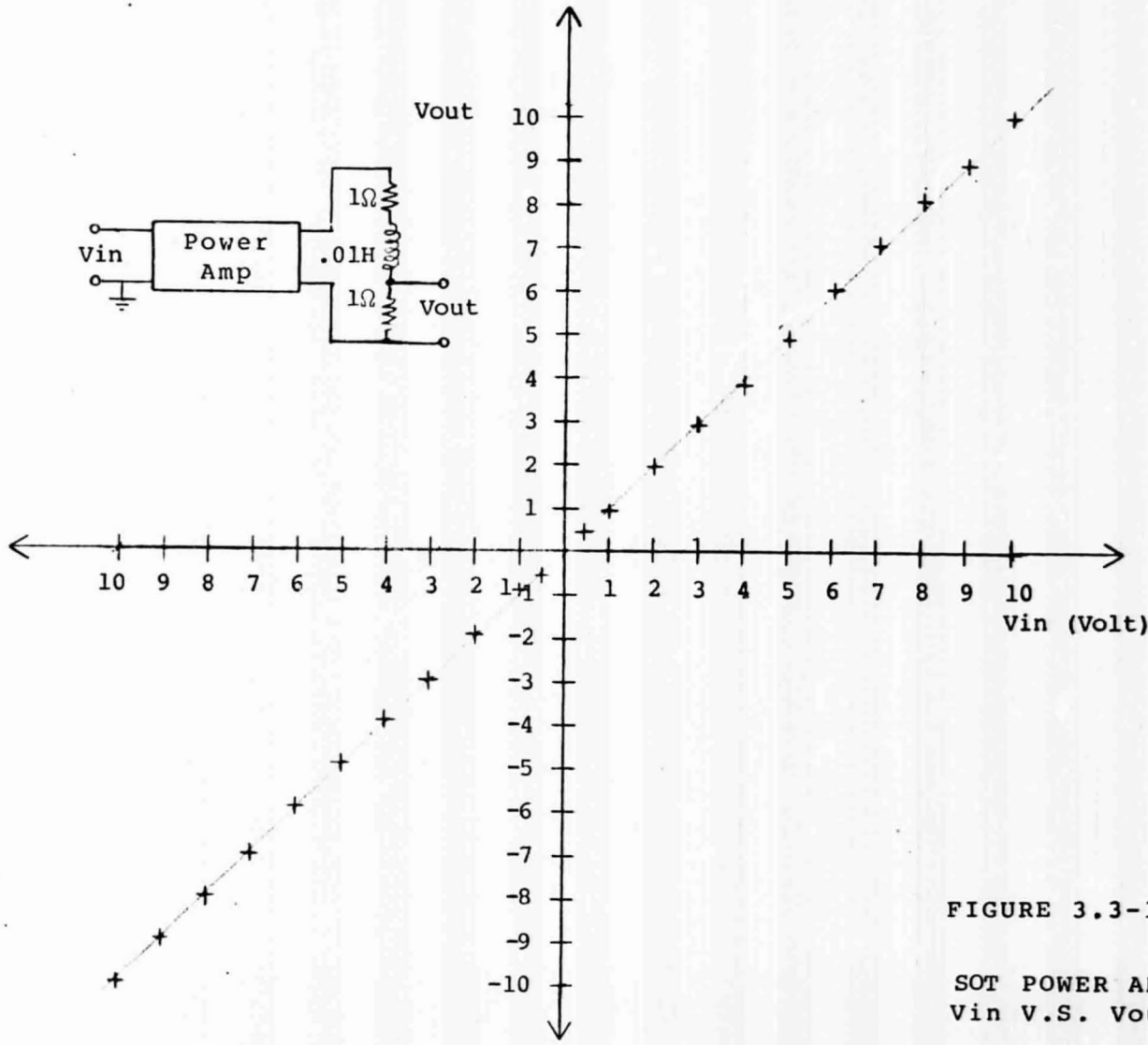

FIGURE 3.3-11

SOT POWER AMP Output Linearity
Vin V.S. Vout (across 1Ω)

4.1 CONCLUSIONS

1. Program results indicate that a single All Digital Controller has sufficient capability to totally handle the computational requirements for control of the SOT APM, including:

    1. All APM control transformations
    2. Control of all 6 actuator loops
    3. Measurement of all 5 sensors
    4. Control of LOS guider or other mechanisms
    5. Miscellaneous housekeeping and other tasks.

Items 4 and 5 were not actually demonstrated but it appears there is sufficient unused capacity of the ADC in performing the first 3 tasks that the additional control tasks could be handled.

2. Present tasks approximately utilize 1/4 of program memory, 1/3 of data memory and 2/3 of the time available. It is felt that time utilized in performing present tasks could be reduced without significantly affecting system performance.

3. The use of the "zero based" "Precision" transformation, from the neutral position of the mirror to its required position, provides a means of holding roll angle at

zero without measuring roll. It also provides an excellent open loop capability which could be most valuable in permitting experiments to continue even with failure of certain sensors.

4. Open loop accuracy of the SOT APM should be approximately .15 arc second, about 6 times better then specified. If additional open loop accuracy is required it can be achieved.

5. A "model reference" control technique has been defined which provides precision control while minimizing excitation of structural modes. The approach is flexible in permitting adjustments to parameters should unexpected structural resonances or other problems be encountered.

6. The use of tachometers in a tight analog loop around the control actuator combined with increased inertia make possible tight control while minimizing excitation of structural modes.

7. The power amplifier designed for the SOT application has not as yet been demonstrated. Because of the use of pulse width modulation within a wide-band analog loop, plus the use of new VMOS transistors whose full capabilites are yet being explored, this is an area of risk. (NASA suggested use of VMOS for this application as an exploratory means of evaluating their capability. Considerable power savings can be achieved through their use. Navtrol agreed and continues to agree with their

use on this "breadboard" system.)

8. The encoder interface approach developed by Navtrol for use on SOT offers a way of achieving very high resolution, required in control applications, without sacrificing system reliability. The chance of dropping pulses is minimized by Navtrol's "hard logic" approach to obtaining resolution beyond that provided by the basic number of lines in the encoder.

9. Navtrol believes that one of the major risk areas in the SOT APM control is structural resonances. If these modes are too low in frequency,control bandwidths must be decreased with a subsequent degradation of performance.

4.2 RECOMMENDATIONS

1. It is recommended that the program to construct a mock up of the APM be continued so that control techniques can be tested and evaluated at an early stage in the program to minimize the possiblity of costly delays due to problems encountered with flight hardware.

2. In conjunction with recommendation number 1, it is recommended that Navtrol be funded to continue development of the electronics for the APM mock up system. Initially this will include closed loop tests of a single actuator but eventually should include tests on the overall six actuator system, including sensor

measurements as possible.

3. It is recommended that use be made of the considerable analytical and error analysis capability developed by Navtrol on this program to provide information to NASA and candidate contractors on error sensitivities and performance limitations.

4. It is recommended that each actuator control include use of both a tachometer and an inertia wheel to enable meeting the performance requirement while minimizing the possiblity of exciting structural modes. Increasing the inertia from .014 to .14 in. oz. second^2 does not adversely affect, to a significant degree, the torque requirements of the system.